

AD-A040 417

ARMY ELECTRONICS COMMAND FORT MONMOUTH N J
EVALUATION OF THE NOAA-4 VTPR THERMAL WINDS FOR NUCLEAR FALLOUT--ETC(U)
MAR 77 L D DUNCAN, M A SEAGRAVES

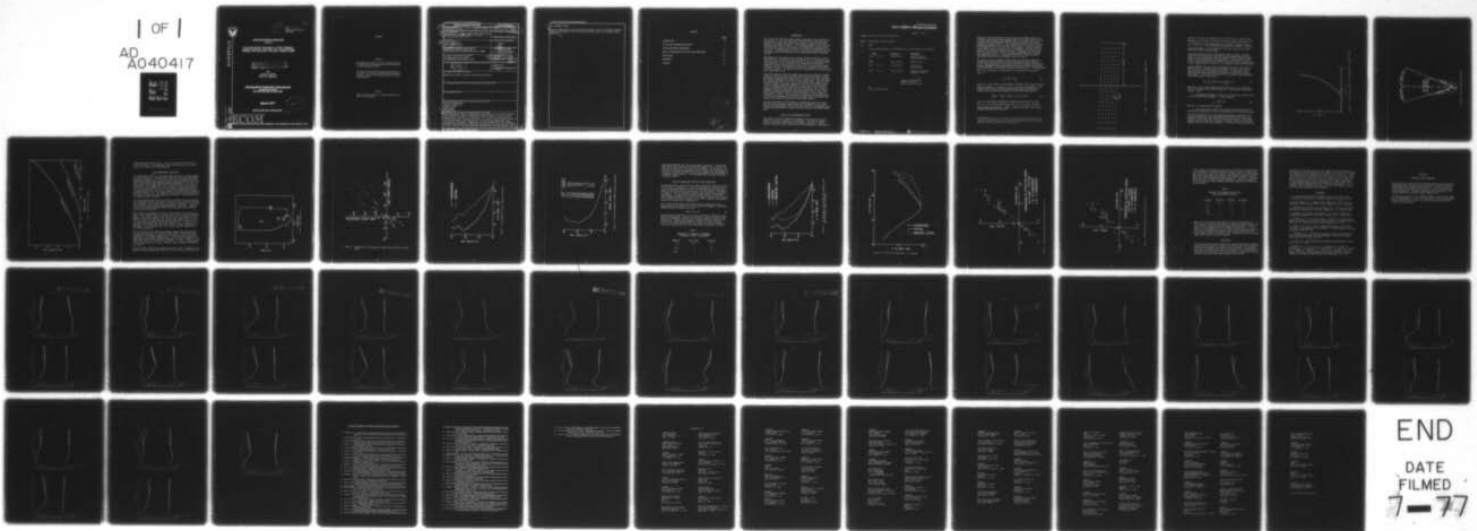
F/G 18/3

UNCLASSIFIED

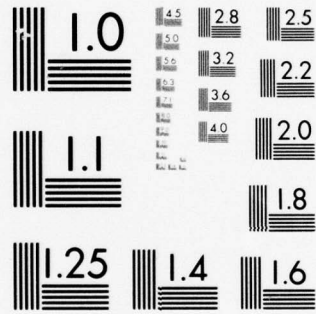
ECOM-5815

NL

| OF |
AD
A040417



END
DATE
FILMED
7-77



MICROCOPY RESOLUTION TEST CHART
NATIONAL BUREAU OF STANDARDS-1963-A



12

9

AD

Reports Control Symbol
OSD-1366

RESEARCH AND DEVELOPMENT TECHNICAL REPORT
ECOM-5815

EVALUATION OF THE NOAA-4 VTPR THERMAL WINDS FOR NUCLEAR FALLOUT PREDICTIONS

COPY AVAILABLE TO DDC DOES NOT
PERMIT FULLY LEGIBLE PRODUCTION

By
Louis D. Duncan
Mary Ann Seagraves

Atmospheric Sciences Laboratories

US Army Electronics Command
White Sands Missile Range, New Mexico 88002

March 1977

Approved for public release; distribution unlimited.

DDC
RECEIVED
JUN 10 1977
A

ADA 040417

DDC FILE COPY

ECOM

UNITED STATES ARMY ELECTRONICS COMMAND - FORT MONMOUTH, NEW JERSEY 07703

NOTICES

Disclaimers

The findings in this report are not to be construed as an official Department of the Army position, unless so designated by other authorized documents.

The citation of trade names and names of manufacturers in this report is not to be construed as official Government indorsement or approval of commercial products or services referenced herein.

Disposition

Destroy this report when it is no longer needed. Do not return it to the originator.

SECURITY CLASSIFICATION OF THIS PAGE (When Data Entered)

REPORT DOCUMENTATION PAGE		READ INSTRUCTIONS BEFORE COMPLETING FORM	
14 1. REPORT NUMBER ECOM-5815	2. GOVT ACCESSION NO.	3. RECIPIENT'S CATALOG NUMBER (9) Research and Development Technical Rept.	
6 4. TITLE (and Subtitle) EVALUATION OF THE NOAA-4 VTPR THERMAL WINDS FOR NUCLEAR FALLOUT PREDICTIONS.	5. TYPE OF REPORT & PERIOD COVERED		
7. AUTHOR(s) Louis D. Duncan Mary Ann Seagraves		8. CONTRACT OR GRANT NUMBER(s)	
9. PERFORMING ORGANIZATION NAME AND ADDRESS Atmospheric Sciences Laboratory White Sands Missile Range, New Mexico 88002		10. PROGRAM ELEMENT, PROJECT, TASK AREA & WORK UNIT NUMBERS DA Task 1T162111AH71A267	
11. CONTROLLING OFFICE NAME AND ADDRESS US Army Electronics Command Fort Monmouth, New Jersey 07703		12. REPORT DATE March 1977	173
14. MONITORING AGENCY NAME & ADDRESS (if different from Controlling Office) (12) 44p.		13. NUMBER OF PAGES 48	1A2
		15. SECURITY CLASS. (of this report) UNCLASSIFIED	
		15a. DECLASSIFICATION/DOWNGRADING SCHEDULE	
16. DISTRIBUTION STATEMENT (of this Report) Approved for public release; distribution unlimited.			
17. DISTRIBUTION STATEMENT (of the abstract entered in Block 20, if different from Report)			
18. SUPPLEMENTARY NOTES			
19. KEY WORDS (Continue on reverse side if necessary and identify by block number) Satellite meteorology Fallout prediction Thermal winds Meteorology Wind profiles			
20. ABSTRACT (Continue on reverse side if necessary and identify by block number) The procedure and theory for determining wind profiles from radiance measurements obtained by vertical temperature profile sounders on polar orbiting meteorological satellites are presented. The use of the wind profiles from 15 to 30 km altitude in the generation of nuclear fallout prediction on the battlefield is discussed. Comparisons of winds obtained with this technique with profiles obtained from radiosonde measurements have been made for 33 sets of data. Results of these comparisons indicate that the winds derived from			

20. ABSTRACT (cont)

radiance measurements are sufficiently accurate to satisfy the Army's requirements for wind data, in the 15 to 30 km altitude range, for nuclear fallout prediction.

INTRODUCTION

On 16 July 1945, the first atomic bomb was exploded in the Southern New Mexico desert. From this experience, and others which followed, man has begun to realize the necessity for protection against the harmful effects of an atomic explosion. These effects include initial radiation, heat and blast effects, shock waves, and contamination resulting from the fallout of radioactive particles carried into the atmosphere by the explosion. Protection against fallout is available through both the use of shelters and from predictions of the time and location of hazardous fallout.

Requirements for the generation of nuclear fallout predictions on the battlefield are discussed in several documents [1-4]. The primary meteorological input is the wind data obtained by the radio-tracked balloonsonde soundings (usually referred to as radiosonde or rawinsonde soundings) of the upper atmosphere made by the US Army Artillery Meteorological Sections. Soundings to at least 30 km altitude are required at 6-hour intervals. No other battlefield requirements for meteorological data extend above 15 km.

The nuclear fallout prediction capability has been on readiness standby status for the past 30 years and has exerted a distinct impact on Army battlefield meteorological operations as a result of the data collection and analysis necessary for nuclear fallout predictions. The requirement for balloonsonde data in the 15 to 30 km altitude range imposes a substantial increase (over that required for the 0 to 15 km observations) in meteorological equipment, operations, and man-hours on the battlefield. The Meteorological Satellite Technical Area of the US Army's Atmospheric Sciences Laboratory (ASL) has conducted an active research program to develop applications of meteorological data to upper level winds (above 15 km) for nuclear fallout prediction. This program is referred to as SATFAL. This research has demonstrated that meteorological satellite measurements can provide the upper level winds more efficiently than currently operational balloonsonde systems.

The basic principles and techniques for determining upper level winds from satellite radiometric measurements are presented in this report. Results from measurements made by the NOAA-4 satellite are compared with balloonsonde measurements to demonstrate and evaluate the SATFAL capabilities.

SATFAL WIND DETERMINATION THEORY

The advent of vertical temperature soundings from satellites has provided a new tool for atmospheric measurements. The thermal sounder is a passive instrument which senses the outgoing radiances in several spectral intervals as seen from the top of the atmosphere. The vertical

DEFENSE SUPPLY AGENCY

Inter-Office Memorandum

DATE: 22 Jun 77

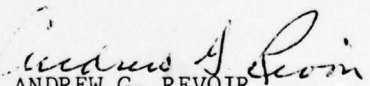
SUBJECT: Renewal of DDC Key Custodian List

FROM : DDC-TA (Mrs. Cornelius/46821)

TO : DDC-T

The following employees are designated as key custodians and alternates

<u>Room</u>		<u>Principal</u>	<u>Alternate</u>
5A218	No. 62	Andrew Revoir	Nancy Cornelius Raymond Washington
5B405		Minor Oliver	Sharon Lewis
5A256	No. 61	Joyce Alford	Jimmie Gray Irving Kelley
5B478	No. 17	Gordon Willey	Eleanor deChadenedes Thurmond A. Long


ANDREW G. REVOIR
Chief, Analysis Division

cc:
Above listed employees



Temperature Profile Radiometer (VTPR)* flown on the NOAA satellites is a thermal sounder which scans perpendicular to the orbital path in order to obtain data extending approximately 1000 km to either side of the subsatellite track (Figure 1). The radiances measured by the VTPR are integrated signatures of the thermal structure in the vertical column of the atmosphere in the field of view of the sounder. The basic physical theory which relates the radiance to the temperature structure is contained in the radiative transfer equation. Algorithms have been developed which allow one to "invert" the radiance measurements and obtain the temperature profiles. A temperature profile, if desired, may be determined at each of the grid points shown in Figure 1.

The use of satellite measured radiance data to calculate a usable approximation of the wind field has been discussed by several authors [5-7]. These observations have been based upon well-known relationships between atmospheric thermal and dynamic structures with the wind given by the geostrophic wind through the thermal wind equation. The geostrophic wind, \vec{V}_g , is given by (cf Holton [8] for a derivation of this equation)

$$\vec{V}_g = \frac{1}{\rho f} \vec{k} \times \vec{\nabla}_h p \quad (1)$$

where \vec{k} is a unit vector in the vertical direction, $\vec{\nabla}_h p$ is the horizontal pressure gradient, ρ is density, and f is the Coriolis parameter. The vertical shear (derivative) of the geostrophic wind is given by the thermal wind which may be expressed in finite difference form by

$$\vec{V}_g(P_2) - \vec{V}_g(P_1) = \frac{R}{f} \vec{k} \times \vec{\nabla}_p \bar{T} \ln(P_1/P_2) \quad (2)$$

where \bar{T} is the average temperature between pressure levels P_1 and P_2 ($P_2 < P_1$), R is the gas coefficient for dry air, and $\vec{\nabla}_p \bar{T}$ is the horizontal temperature gradient. (NOTE: Pressure and height are related through the hydrostatic equation.)

*A detailed discussion of the VTPR together with operational data processing procedures used by the National Environmental Satellite Service (NESS) is given by McMillian et al. [9] (1973).

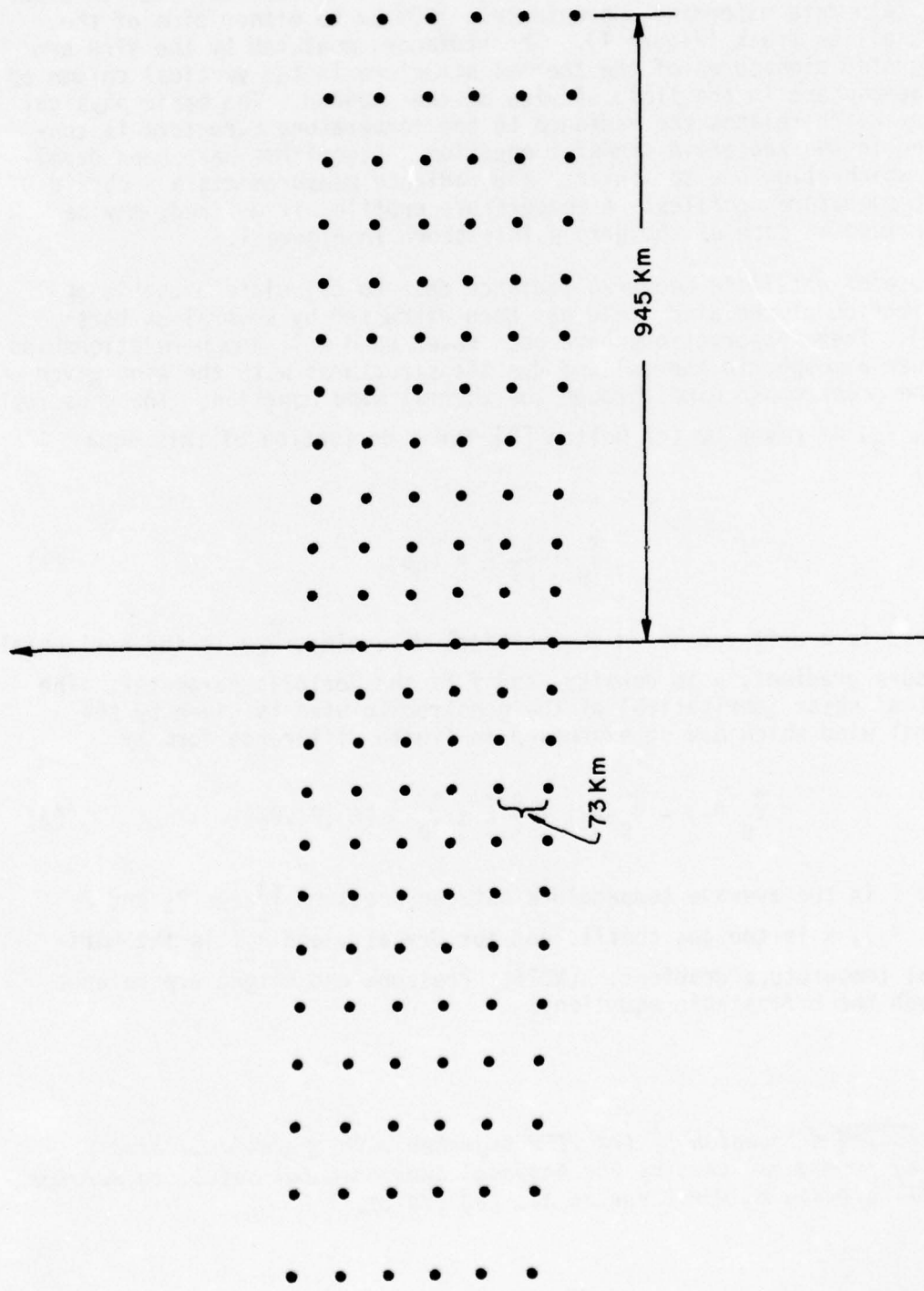


Figure 1. Distribution of Earth Scan Scene for the NOAA-4 VTPR.

Equation (2) shows that determination of the wind at P_2 requires only knowledge of the wind at P_1 and the horizontal temperature gradient $\vec{\nabla}_h \bar{T}$. This procedure can be extended through a sequence of pressure levels $P_1 > P_2 > \dots > P_n$. This is the basic concept used in SATFAL. A balloon-sonde measurement is used to provide the "tie-on" value at the lowest level (at or near 15 km altitude).

The relatively dense grid of observations shown in Figure 1 provides sufficient data for numerical estimation of the temperature gradients. However, as is typical with numerical differentiation problems, considerable care must be taken in this computation. After much trial and error, it was determined that sufficient accuracy could be obtained from a least squares planar fit over a 7 x 7 rectangular array of observations.

Complete details for the fallout predictions are given in TM 3-210 [3] and FM 3-22 [4]. Relevant physical parameters such as nuclear burst time, location, and yield are assumed known. (A discussion of the methods by which this information is obtained is outside the scope of this report.) The effect of wind drift is calculated from the effective wind profile which is defined by

$$\vec{V}(z) = \int_0^z [\vec{U}(\mu)/\tau(\mu)] d\mu / \int_0^z d\mu/\tau(\mu) \quad (3)$$

where $\vec{U}(\mu)$ is the actual (measured) wind profile and $\tau(\mu)$ is the fall rate for a nominal size particle (Figure 2). The principal predictands (Figure 3) are:

a. The downrange distance, R , which is related to the nuclear yield, Y , and the effective windspeed, V , by the expression

$$R = AY^{2/5} V^{1/2} \quad (4)$$

where A is a proportionality constant.

b. The right and left radial lines which are determined from the effective wind directions at the 2/3 stem height and the cloud top height.

The fallout prediction for a specified yield becomes a function of the effective windspeed at the cloud bottom height and the effective wind direction at the cloud top height and the 2/3 stem height. These three heights, which are functions of yield, are shown in Figure 4 for yields ranging from 10 kilotons to 10 megatons. (The data for constructing this

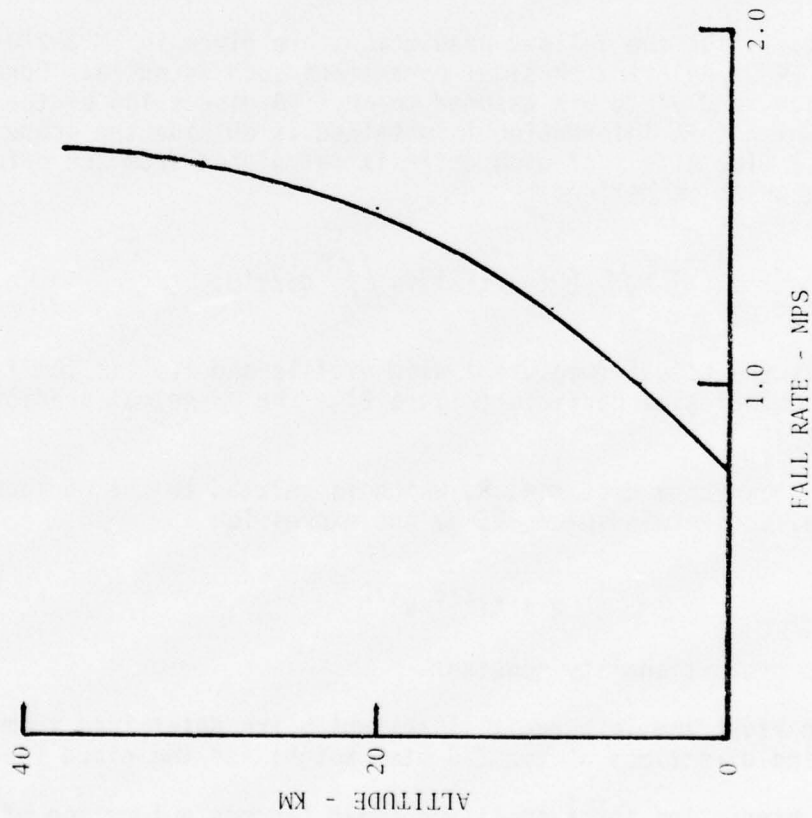


Figure 2. Fall rate for nominal fallout particles - source FM 3-22.

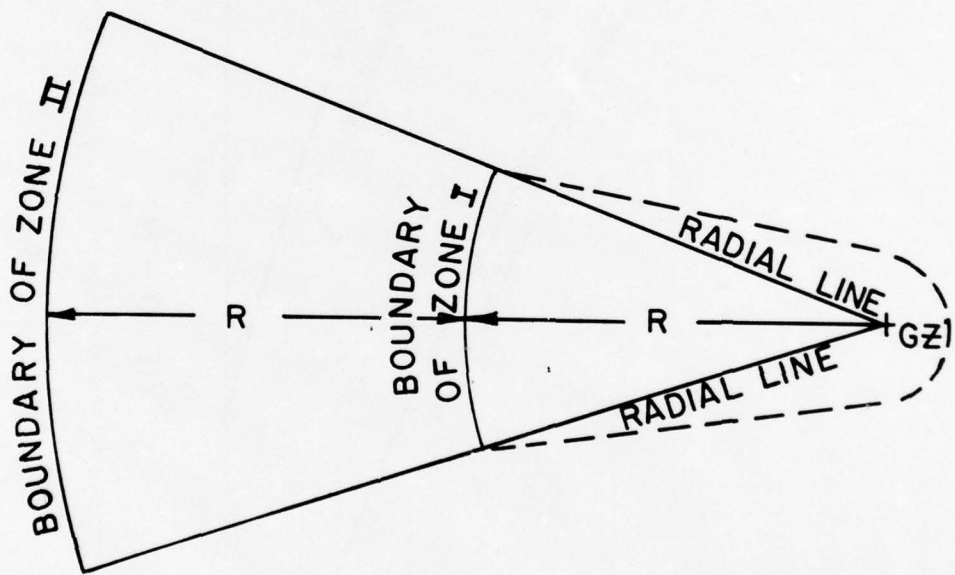


Figure 3. Fallout prediction diagram.

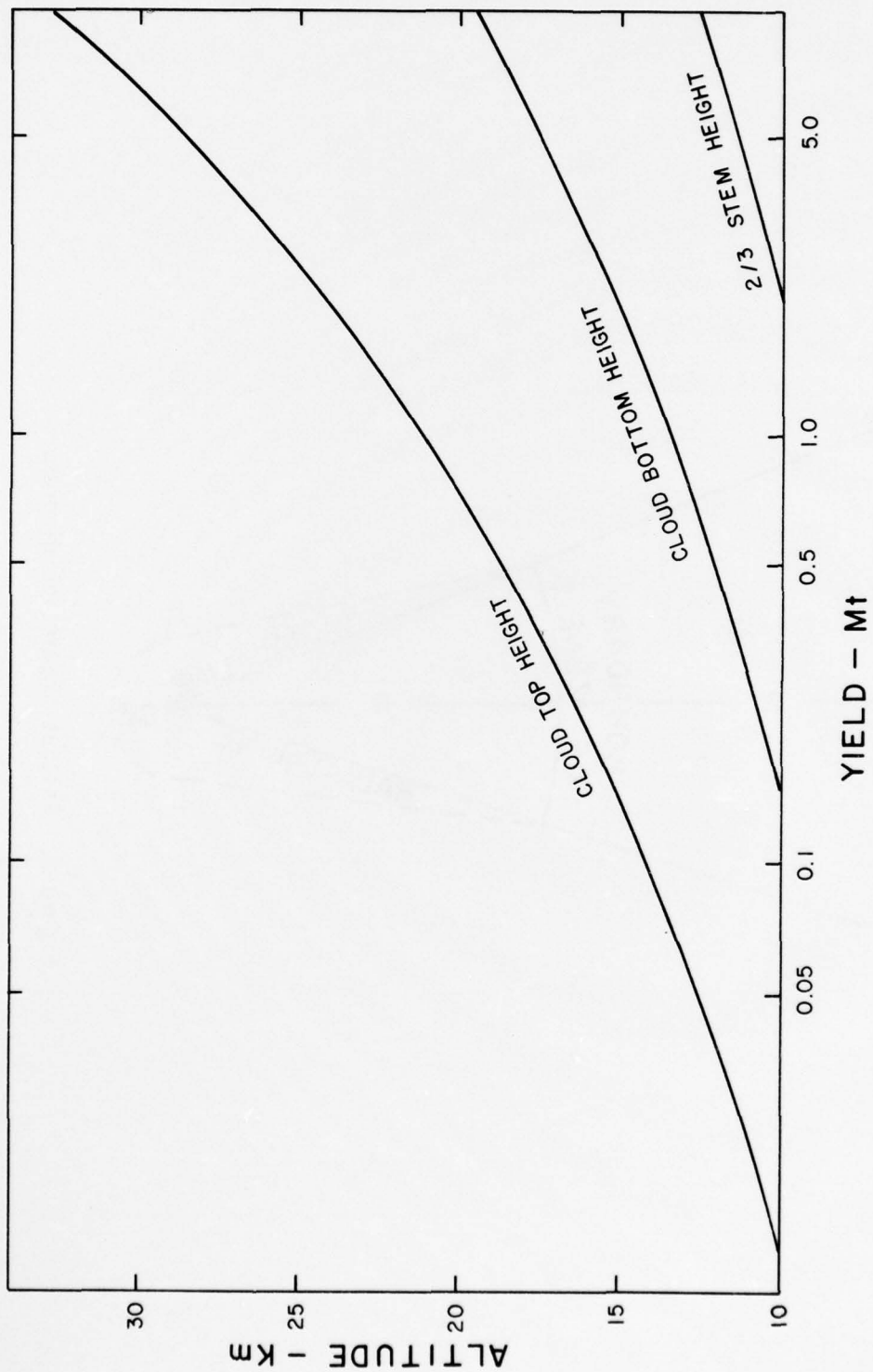


Figure 4. Nuclear cloud height parameters.

graph were taken from TM 3-210.) Only the direction of the effective wind is required for altitudes above the cloud bottom height, which is generally a rather large altitude range.

SATFAL/RADIOSONDE COMPARISONS

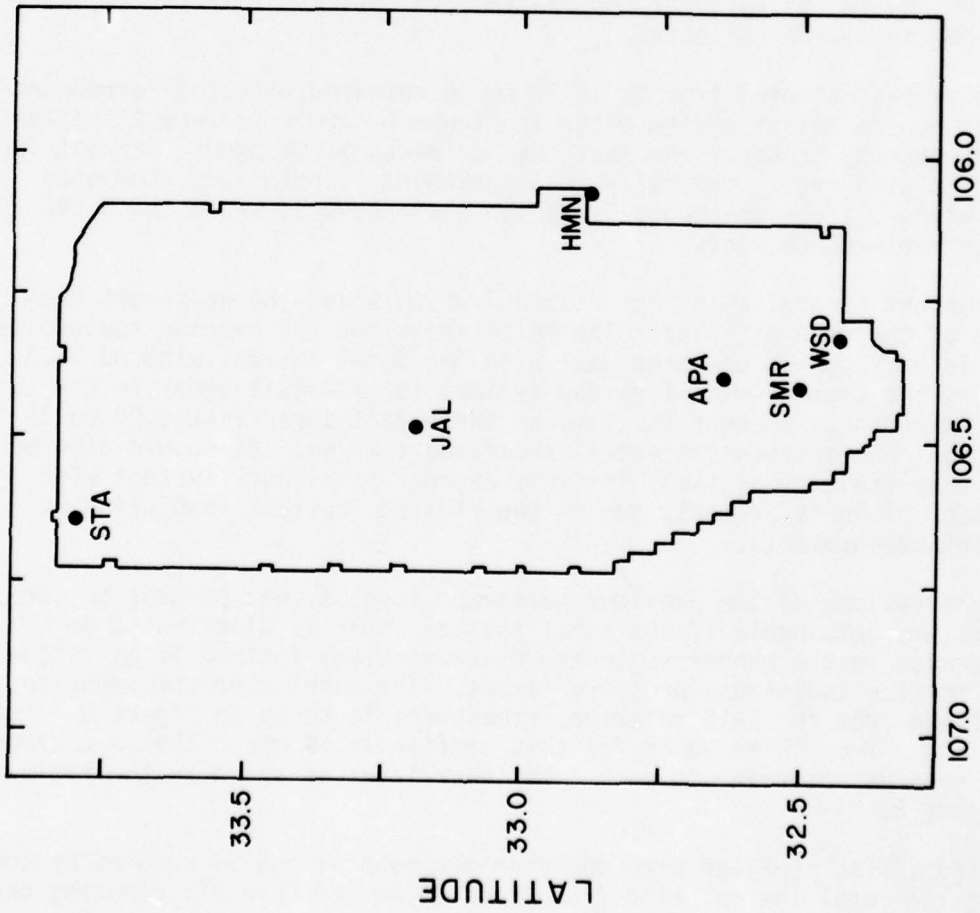
Six radiosonde stations are located on White Sands Missile Range (WSMR), New Mexico (Figure 5). A special data collection was conducted between February and December 1975 to obtain a data base for SATFAL evaluation. Radiosonde balloons were launched (nearly) simultaneously from the three lower range stations (WSD, SMR, and HMN) approximately 1 hour prior to the passover of the NOAA-4 satellite. (The release time was chosen to minimize the time variability of the wind data.) Eleven abutting pressure layers extending from 125 to 10 mb (with corresponding altitudes of approximately 15 to 31 km) were selected for thermal wind computations employing Equation (2). The average of the three measured wind profiles was used as "truth" data for comparative evaluation. Thirty-three sets of comparisons were collected.

The total thermal wind from 15 to 30 km is compared with the corresponding radiosonde measured wind shear in Figure 6. Dots represent the east-west component; crosses represent the north-south component. Except for a few isolated cases, generally good agreement is obtained. Computed correlation coefficients were 0.786 for the east-west winds and 0.743 for the north-south winds.

More insight is available from Figure 7 which shows the east-west component of the mean profiles. The total shear for the average radiosonde winds is 18.9, which compares well with the total thermal wind of 16.3. However, the thermal wind lags the typical large actual shear in the 15 to 20 km region, is about the same as the actual shear in the 20 to 25 km region, and exceeds the actual shear above 25 km. It should also be noted that the thermal shear for this average is almost constant with altitude. This is probably due to the limited vertical resolution in the VTPR measurements.

The observations of the previous paragraph suggest that perhaps better results are obtainable if the total thermal shear is distributed percentage-wise in the manner suggested by climatology instead of as calculated for the individual pressure layers. The zonal wind component for WSMR taken from the IRIG reference atmosphere is shown in Figure 8. The total shear from 15 to 30 km for this profile is 19 mps. The percentage of this value occurring in each 1 km thick layer is shown in the table on Figure 8.

Modified SATFAL profiles were computed for each of the 33 samples by computing the total thermal wind from 15 to 30 km and then distributing the



LONGITUDE

Figure 5. WSMR radiosonde sites.

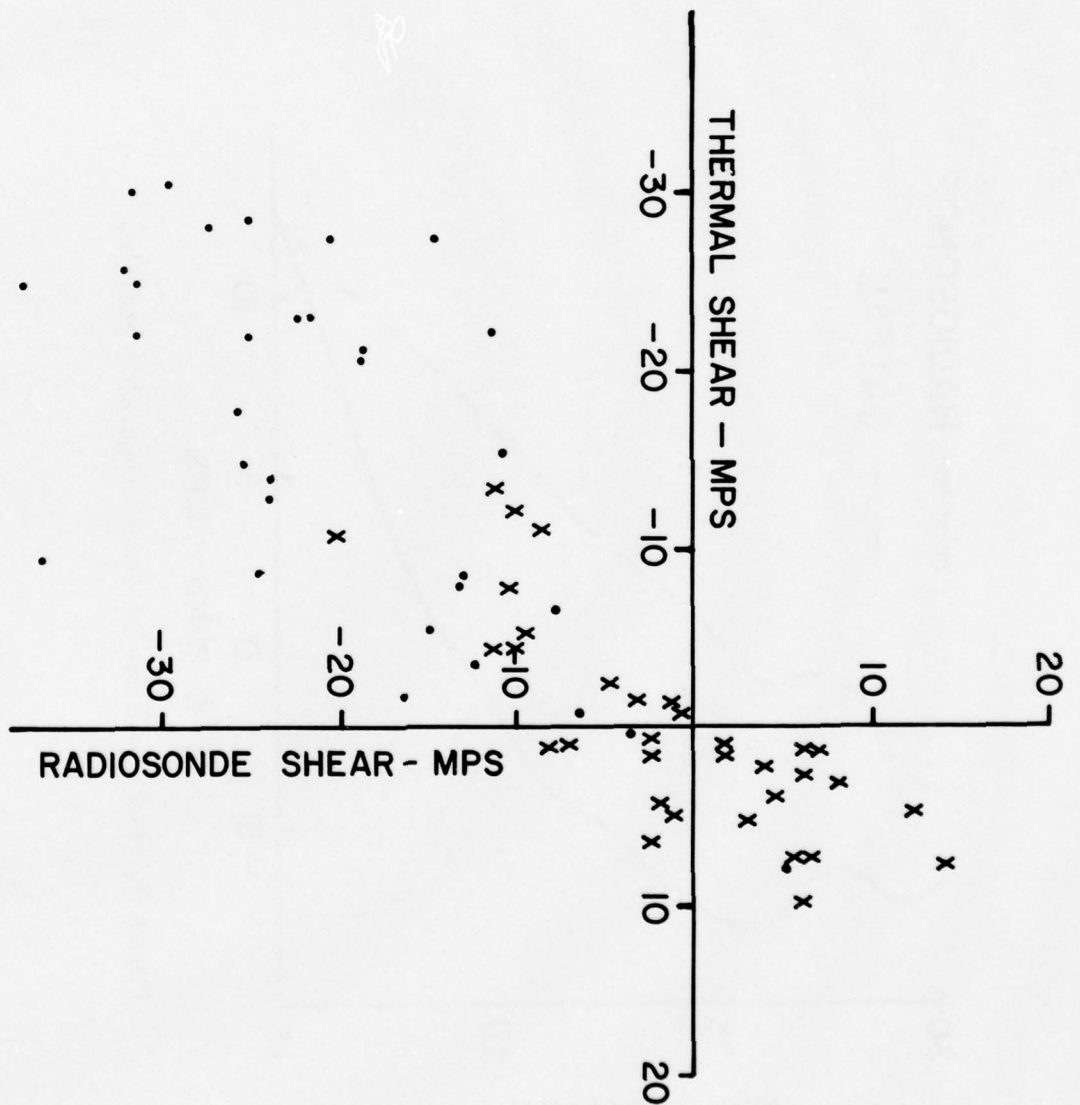


Figure 6. Comparison of radiosonde and thermal shear for the 15-30-km layer.

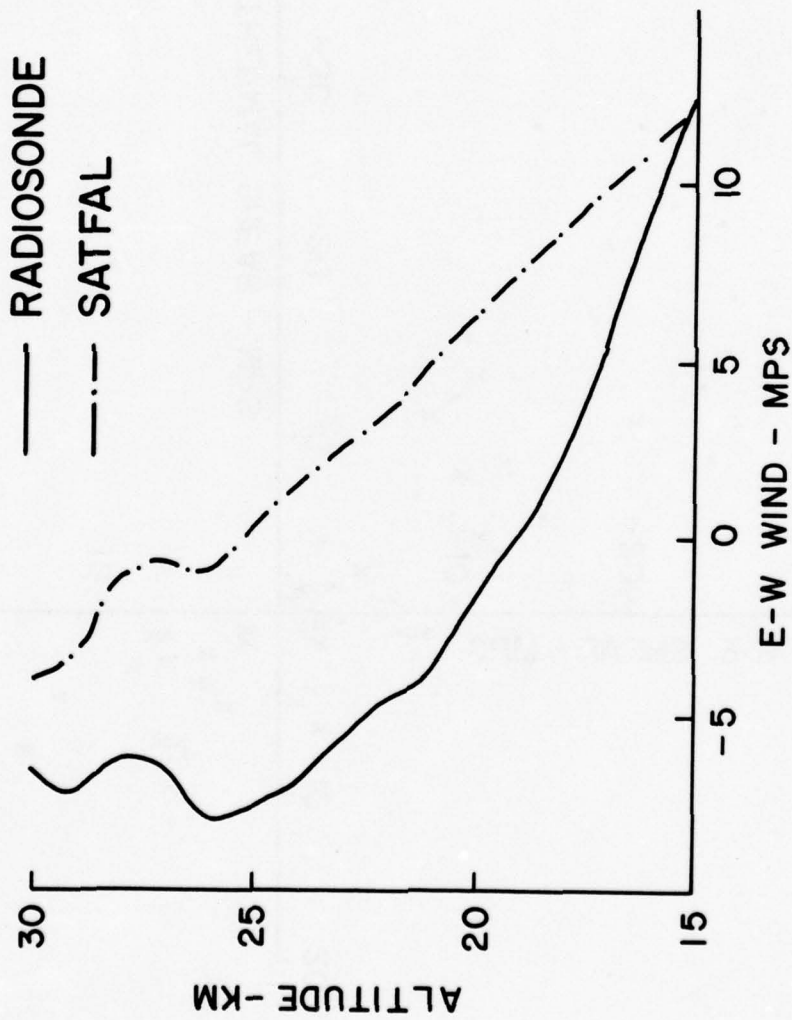


Figure 7. E-W component of the average wind profile.

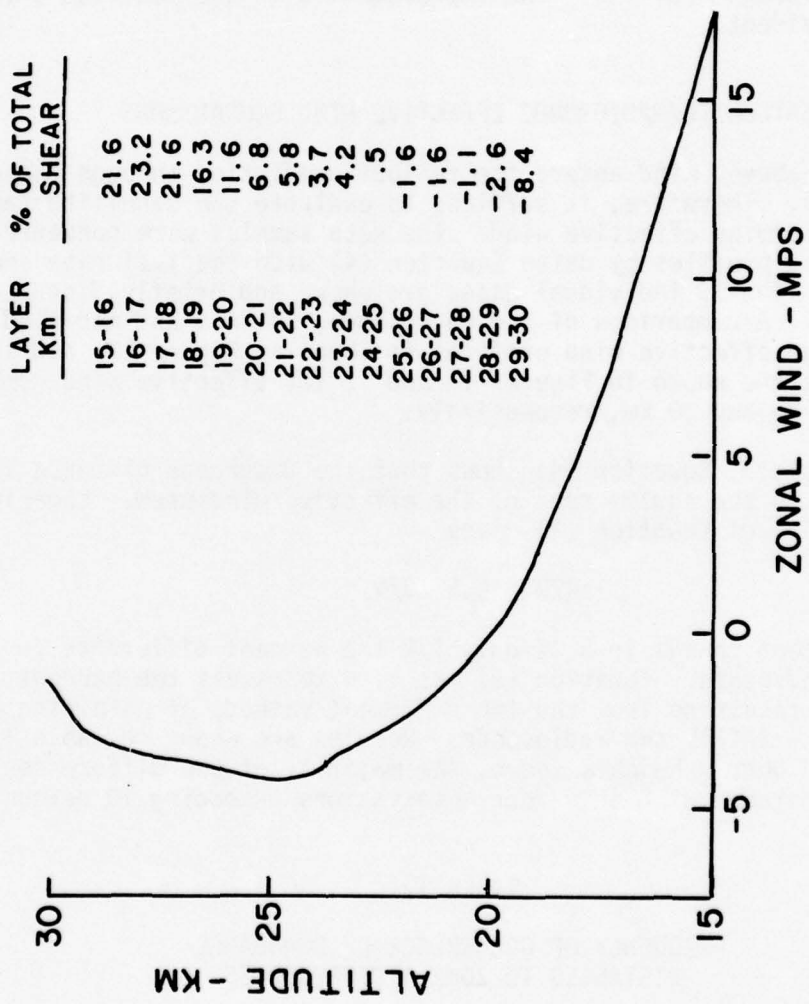


Figure 8. Zonal wind component of WSMR reference atmosphere.

total percentagewise using the values shown in Figure 8. (Through the remainder of this report the term "modified SATFAL" will be used to indicate wind obtained in this manner while "SATFAL" will be used to indicate profiles obtained by using the standard thermal wind computations.) In Figure 9 the modified SATFAL results are compared with the SATFAL and radiosonde average profiles. The improvement with the modified SATFAL is readily evident.

SATELLITE/RADIOSONDE EFFECTIVE WIND COMPARISONS

As discussed above, wind enters the fallout prediction through the effective velocity. Therefore, it suffices to evaluate the satellite capability to determine effective wind. The data samples were converted to effective wind profiles by using Equation (4) with the fall rate shown in Figure 2. The 33 individual cases are shown and briefly discussed in the appendix. A comparison of the radiosonde, SATFAL, and modified SATFAL average effective wind profiles is shown in Figure 10, and statistical results are shown in Figures 11 and 12 for effective wind comparisons at 22.5 km and 30 km, respectively.

For a fixed yield, Equation (4) shows that the downrange distance is proportional to the square root of the effective windspeed. Logarithmic differentiation of Equation (2) gives

$$\Delta R/R = 0.5 \Delta V/V \quad (5)$$

Thus the percent change in R is only 1/2 the percent difference in the effective windspeeds. Equation (5) was used to assess the percent difference in R resulting from the two different methods of obtaining the wind profile - SATFAL and radiosonde. Results are shown in Table 1. For the cloud bottom heights shown, the majority of the differences is less than 5 percent with only four observations exceeding 10 percent.

TABLE 1
FREQUENCY OF OCCURRENCE OF DOWNRANGE
DISTANCES TO ZONE 1 DIFFERENCES

<u>$\Delta R/R$ (%)</u>	<u>at 17.5 km</u>	<u>at 20 km</u>
<5	27	15
5-10	5	14
10-15	1	4

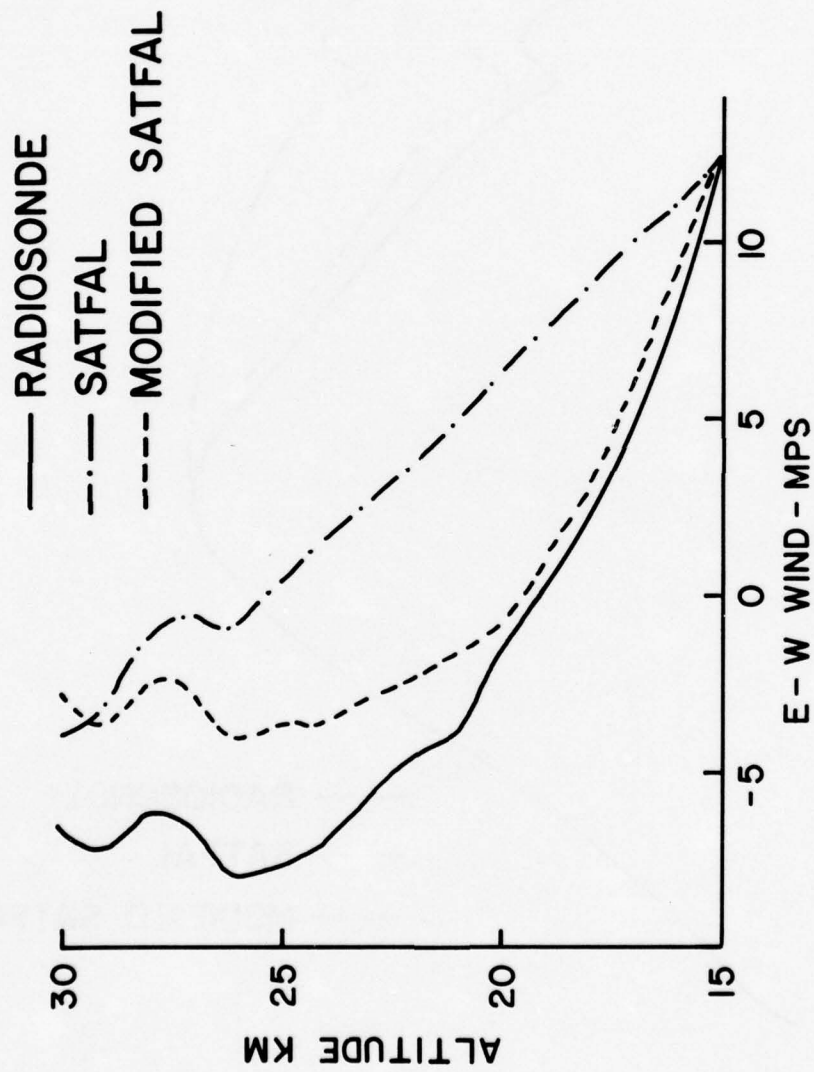


Figure 9. E-W component of the average wind component with modified SATFAL profile included.

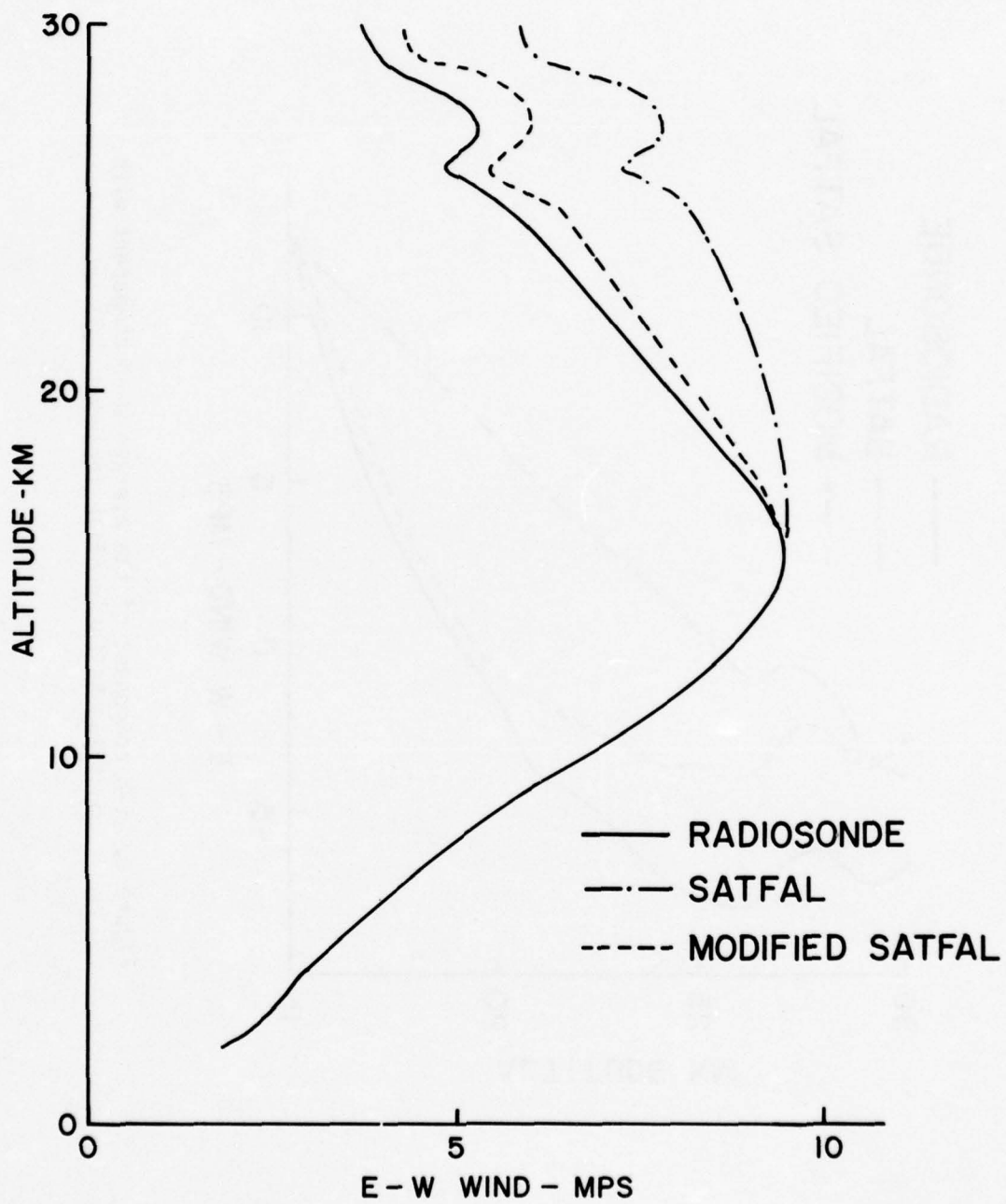


Figure 10. Effective wind comparisons - E-W component.

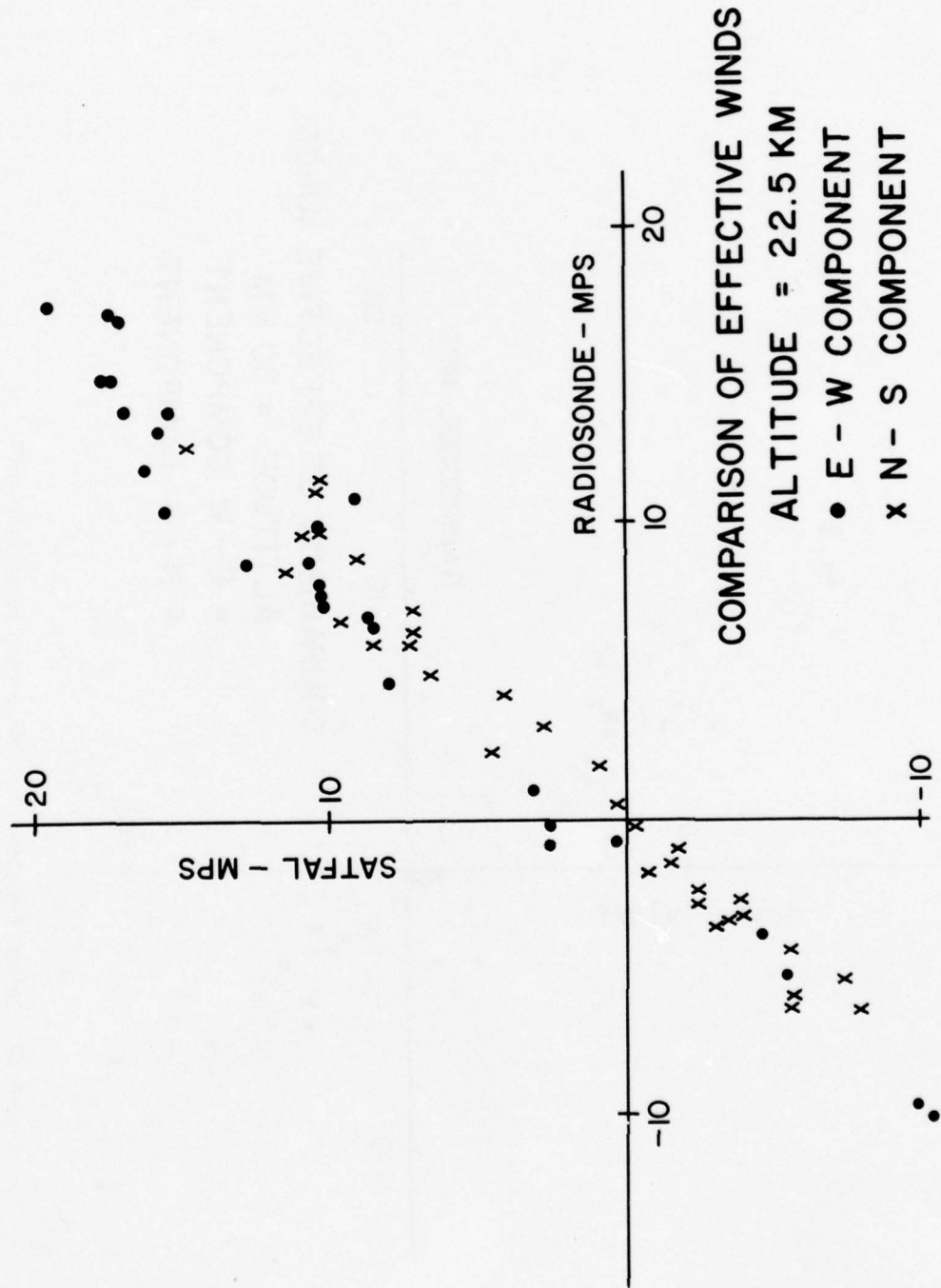


Figure 11. SATFAL/radiosonde effective wind comparison at 22.5 km.

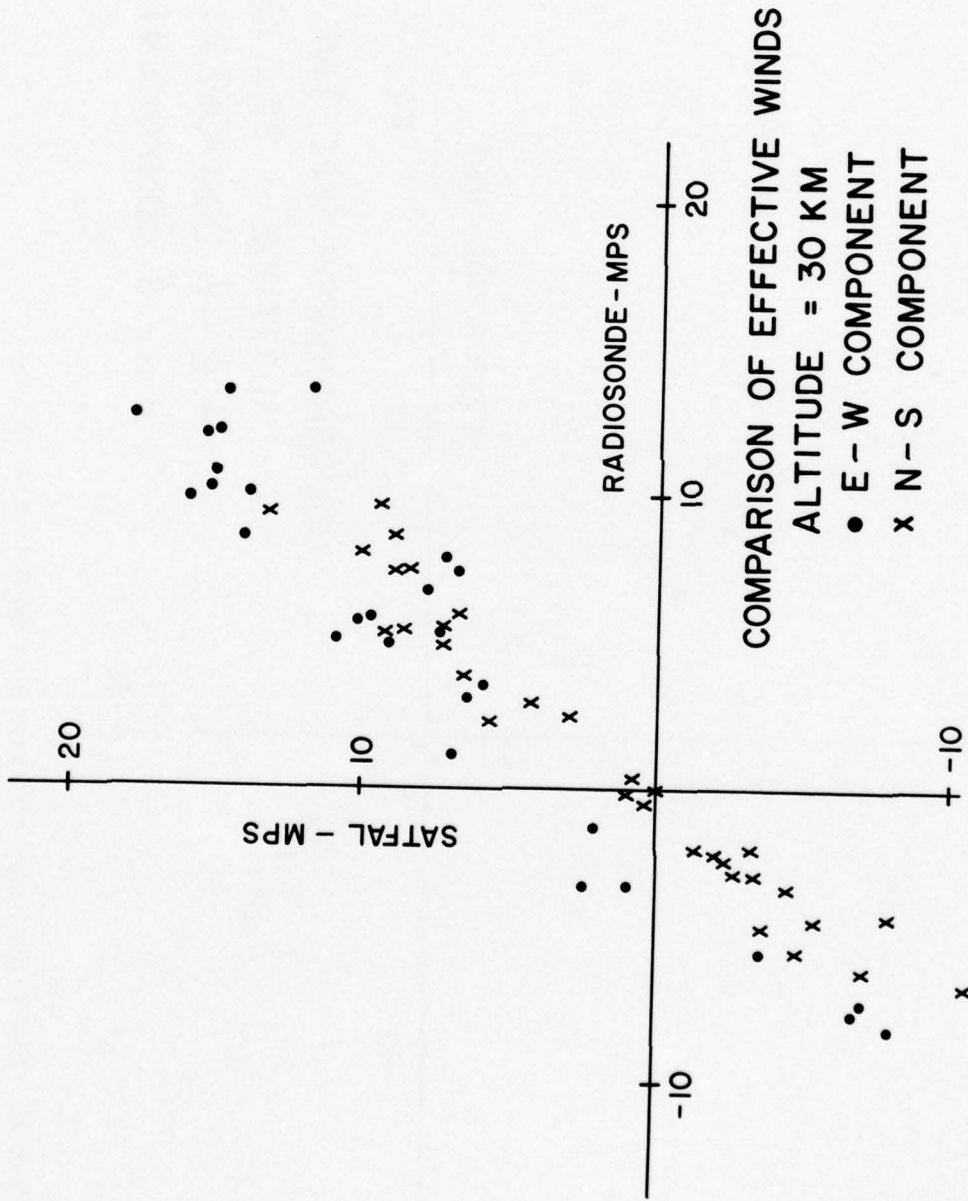


Figure 12. SATFAL/radiosonde effective wind comparison at 30 km.

Table 2 shows the frequency of occurrence of effective wind shear direction differences for three different altitudes. Direction differences are quite small, usually less than 10 and frequently less than 5 degrees. Most of the cases where wind direction differences exceeded 15 degrees were under light windspeed conditions where small changes in the vector wind can result in large direction differences. Very good agreement to 30 km altitude was found in SATFAL/radiosonde comparisons of effective wind direction.

TABLE 2
 FREQUENCY OF OCCURRENCE OF EFFECTIVE
 WIND DIRECTION DIFFERENCES

$\Delta\theta$ (deg)	at 20 km	at 25 km	at 30 km
<5	23	15	14
5-10	7	8	6
10-15	2	4	5
>15	1	6	8

When used in conjunction with Figure 4, the results presented in Tables 1 and 2 show the difference which might be expected between fall-out predictions computed from SATFAL and radiosonde winds. As an example, for an assumed yield of 2.5 megatons (or smaller): (1) the radial line corresponding to the 2/3 stem height would be the same, (2) the percent difference in downrange distance would probably be less than 5 percent, and (3) the radial lines corresponding to the cloud top height should agree to within 5 degrees.

CONCLUSIONS

The system discussed herein employs the advanced technology provided by meteorological satellites to provide an efficient means for satisfying the Army's requirements for upper altitude wind data. The procedure and theory for determination of the wind profile from radiance measurements obtained by vertical temperature sounders on polar orbiting meteorological satellites have been presented and discussed.

An analysis of 33 comparisons of winds obtained from radiosonde balloons and satellite radiances measured by the NOAA-4 VTPR shows that the satellite derived winds are adequate for nuclear fallout prediction. It was also shown that the thermal shear is significantly less than the actual shear in the 15 to 20 km level, and this is believed to be a result of the coarse vertical resolution of the satellite sounder. Modification of the computed thermal winds by the addition of climatological data provides improved agreement with the radiosonde measurements. This is apparent from the average case shown as well as from inspection of the individual cases presented in the appendix.

REFERENCES

1. "Army Qualitative Research and Requirements for Nuclear Effects Information FY-76 Edition" (U), SECRET, US Army Nuclear Agency, 1974.
2. AR 115-10/AFR 105-3, "Meteorological Support for the Field Army," Department of the Army and the Air Force, Washington, D.C., June 1970.
3. Department of the Army Technical Manual 3-210, "Fallout Prediction," Headquarters, Department of the Army, Washington, D.C., December 1967.
4. Department of the Army Field Manual F3-22, "Fallout Predictions," Headquarters, Department of the Army, Washington, D.C., October 1973.
5. Elsberry, R. L., J. W. Wright, and F. L. Martin, "An Experimental Method of Determining Ballistic Wind Making Direct Use of SIRS Radiances," FAMOS TM 9-71, Naval Postgraduate School, Monterey, CA, 1971.
6. Duncan, L. D. and M. D. Kays, "Determining Nuclear Fallout Winds from Satellite Observed Spectral Radiances," US Army Atmospheric Sciences Laboratory, WSMR, NM 1974.
7. Alexander, G. D., "Determining Geostrophic Winds Using A Satellite Borne Infrared Radiometer," US Army Atmospheric Sciences Laboratory, White Sands Missile Range, NM, 1975.
8. Holton, J. R., An Introduction to Theoretical Meteorology, Academic Press, New York, 1972.
9. McMillian, L. M., D. Q. Wark, J. M. Siomkajlo, P. G. Abel, A. Werbowetsky, L. A. Lauritson, J. A. Pritchard, D. S. Crosby, H. M. Woolf, R. C. Luehbe, M. P. Weinreb, H. E. Fleming, F. E. Bittner, and C. M. Hayden, "Satellite Infrared Soundings from NOAA Spacecraft," NESS 65, National Environmental Satellite Services, Washington, D.C., 1973

APPENDIX

INDIVIDUAL DATA COMPARISONS

Comparison of the effective velocity determined from the balloonsonde wind measurements and the derived winds from the satellite radiance measurements are presented in Figure A1-A33. The three separate velocity profiles are identified as follows: A cross indicates radiosonde measurements; a triangle indicates SATFAL computations; and a square identifies the modified SATFAL computations.

The data are plotted at 1 km increments between 2 and 30 km MSL (WSMR MSL is approximately 1.25 km). In some cases the radiosonde data terminates below 30 km; in these cases, usable data were not obtained above the altitude shown.

BEST AVAILABLE COPY

12 FEB 75

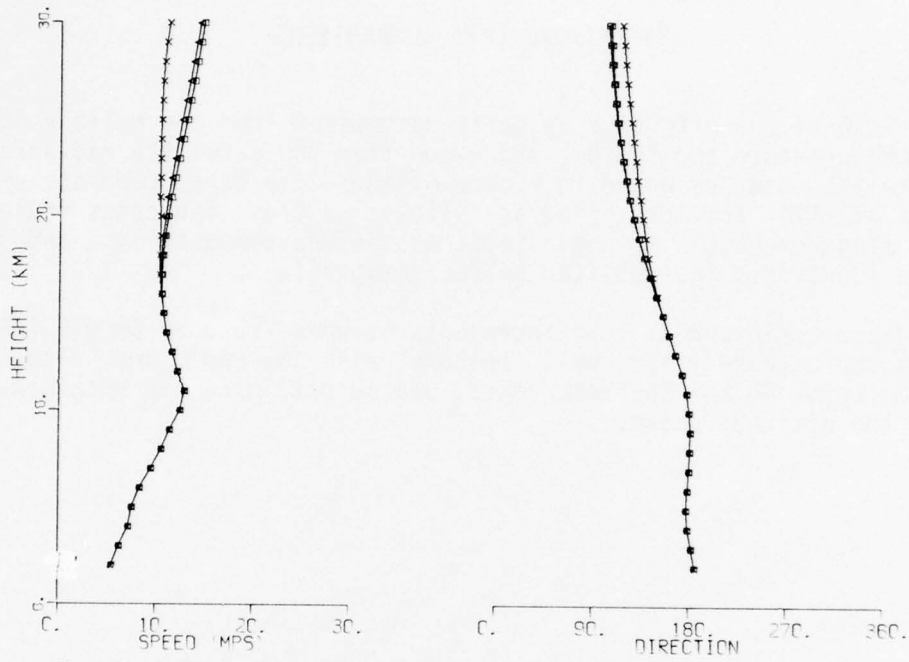


Figure A1. Satellite/radiosonde effective velocity comparison for 12 Feb 75.

20 FEB 75

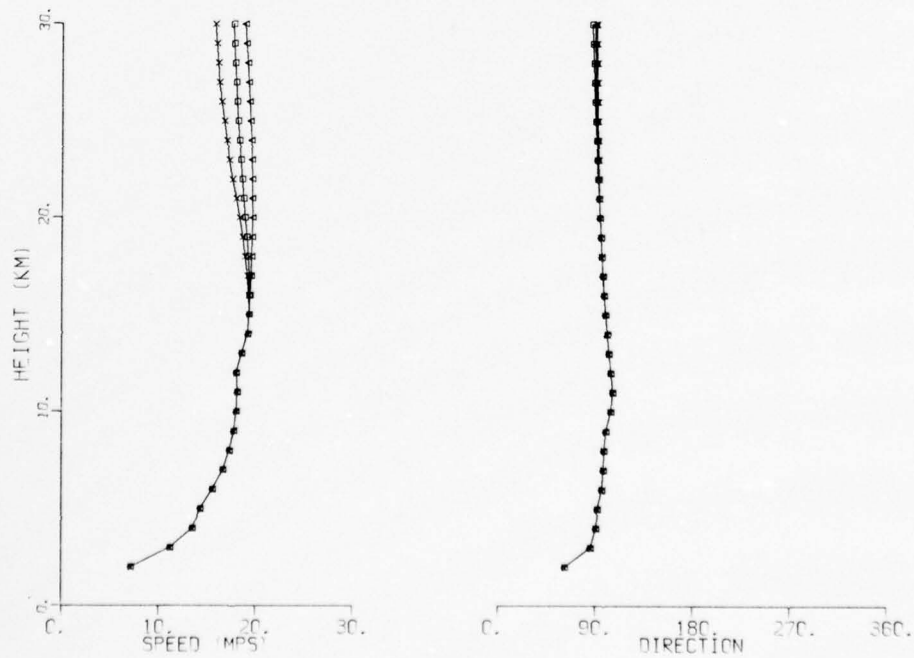


Figure A2. Satellite/radiosonde effective velocity comparison for 20 Feb 75.

BEST AVAILABLE COPY

27 FEB 75

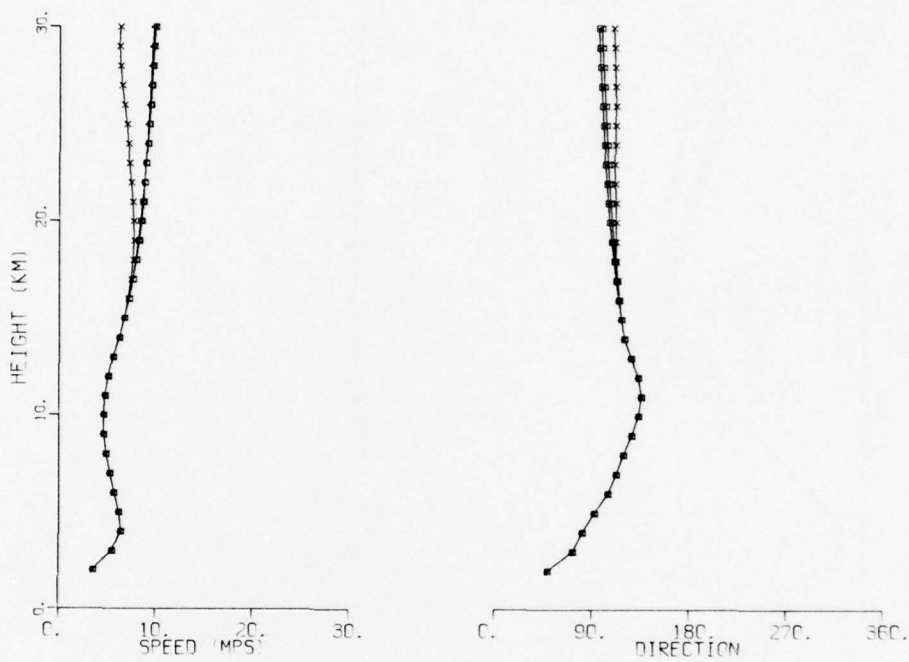


Figure A3. Satellite/radiosonde effective velocity comparison for 27 Feb 75.

28 APR 75

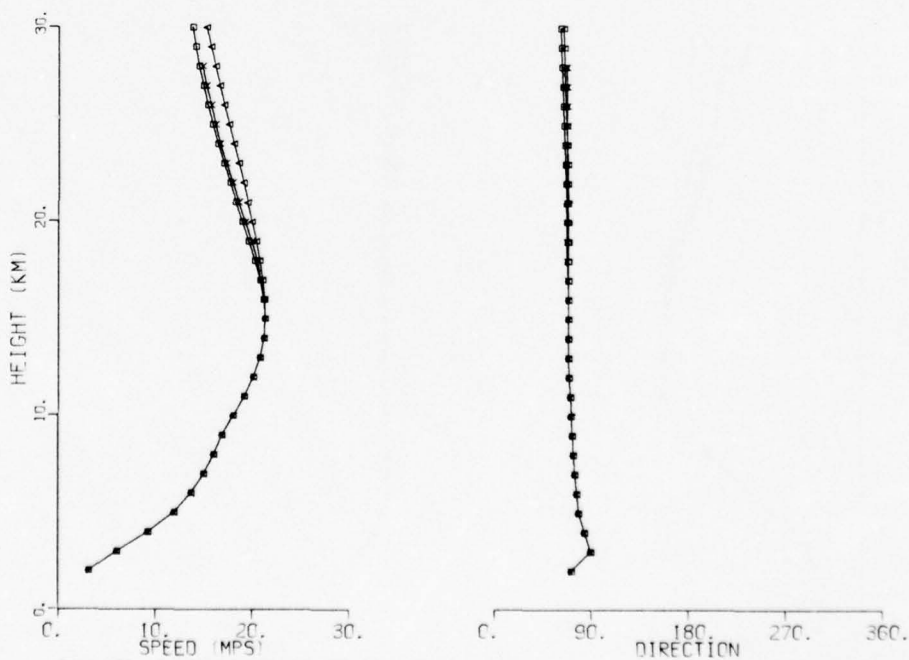


Figure A4. Satellite/radiosonde effective velocity comparison for 28 Apr 75.

BEST AVAILABLE COPY

9 MAY 75

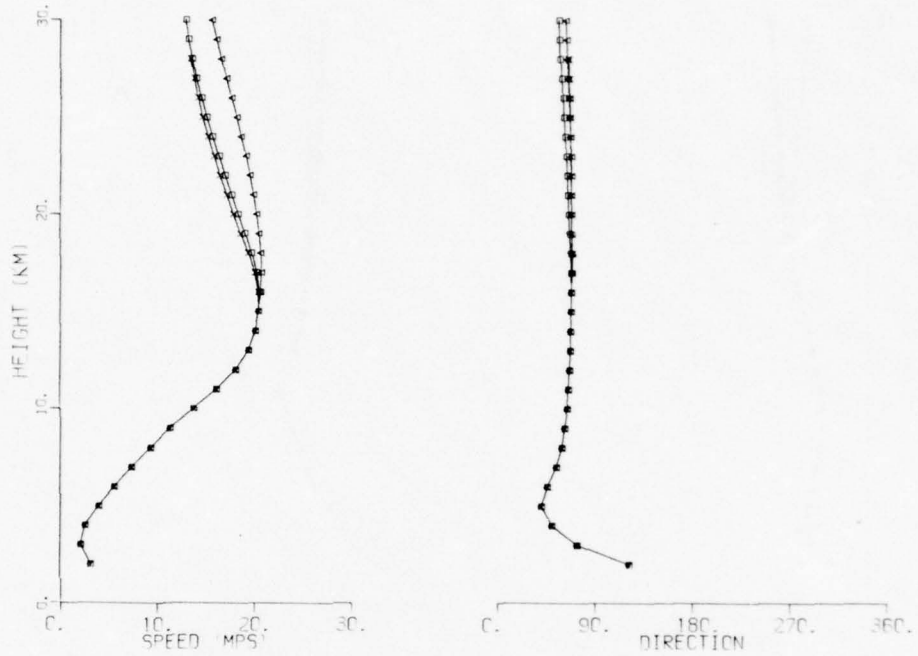


Figure A5. Satellite/radiosonde effective velocity comparison for 9 May 75.

19 MAY 75

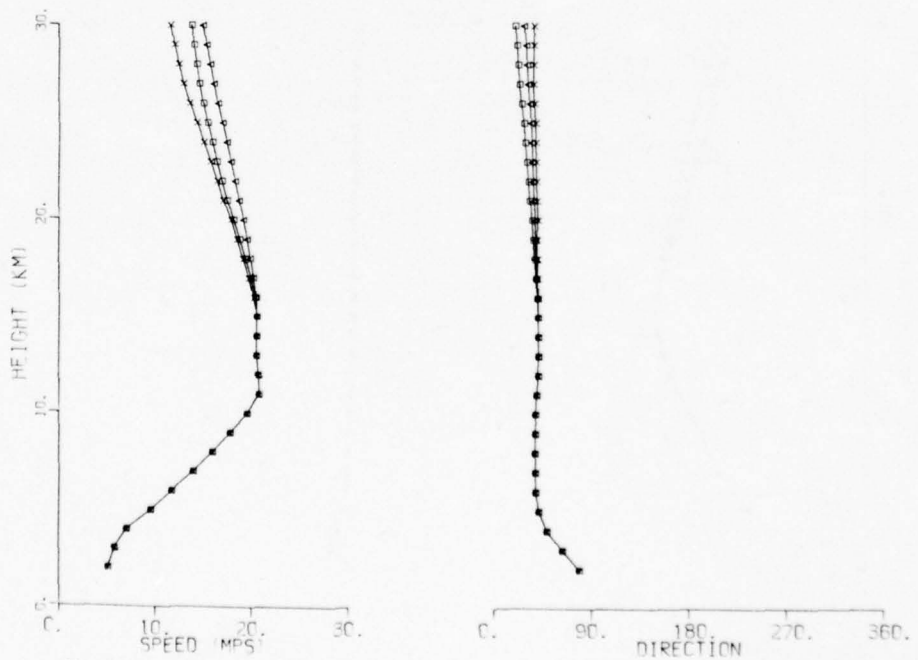


Figure A6. Satellite/radiosonde effective velocity comparison for 19 May 75.

BEST AVAILABLE COPY

21 MAY 75

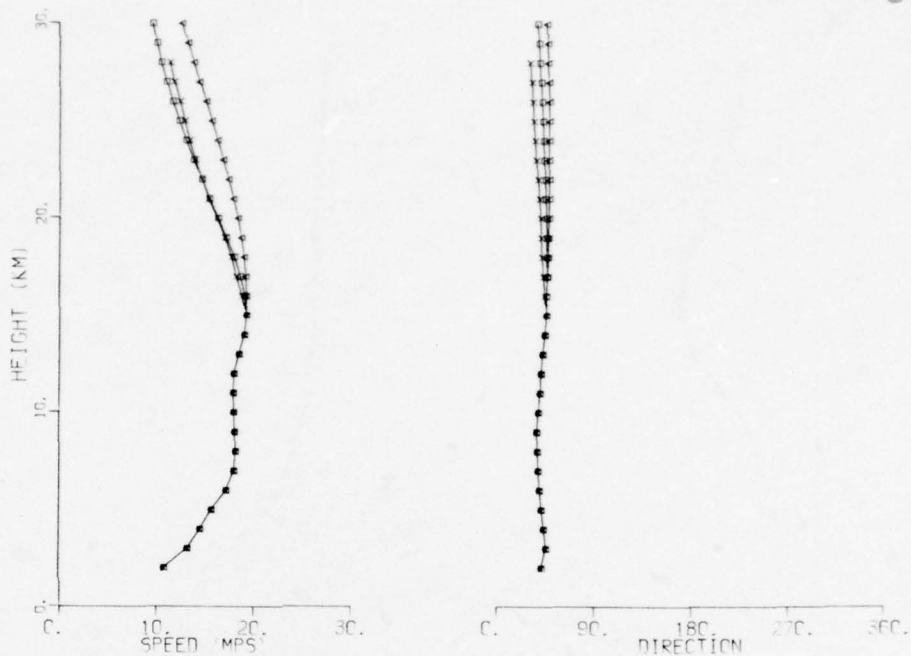


Figure A7. Satellite/radiosonde effective velocity comparison for 21 May 75.

23 MAY 75

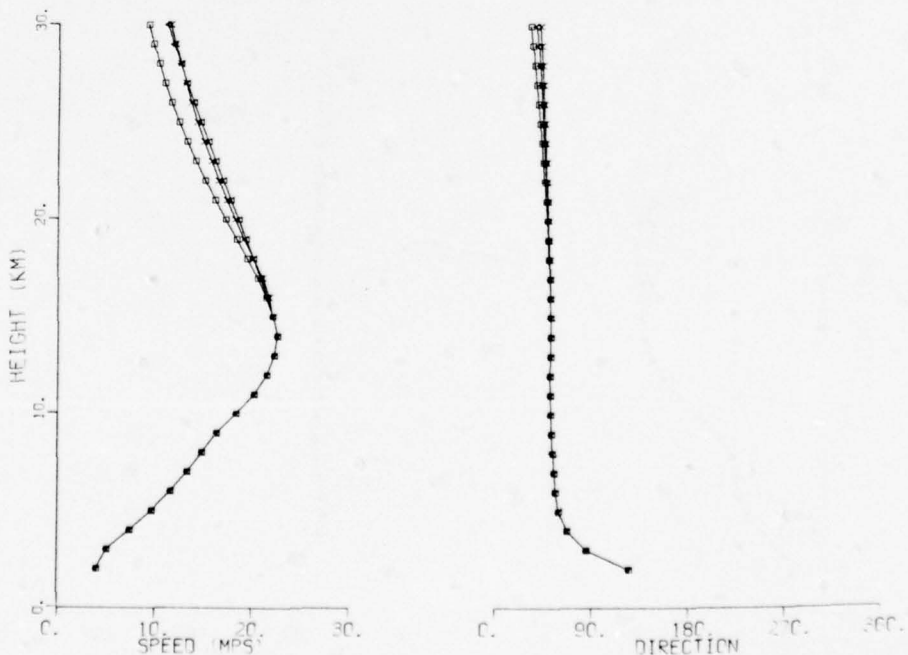


Figure A8. Satellite/radiosonde effective velocity comparison for 23 May 75.

9 JUN 75

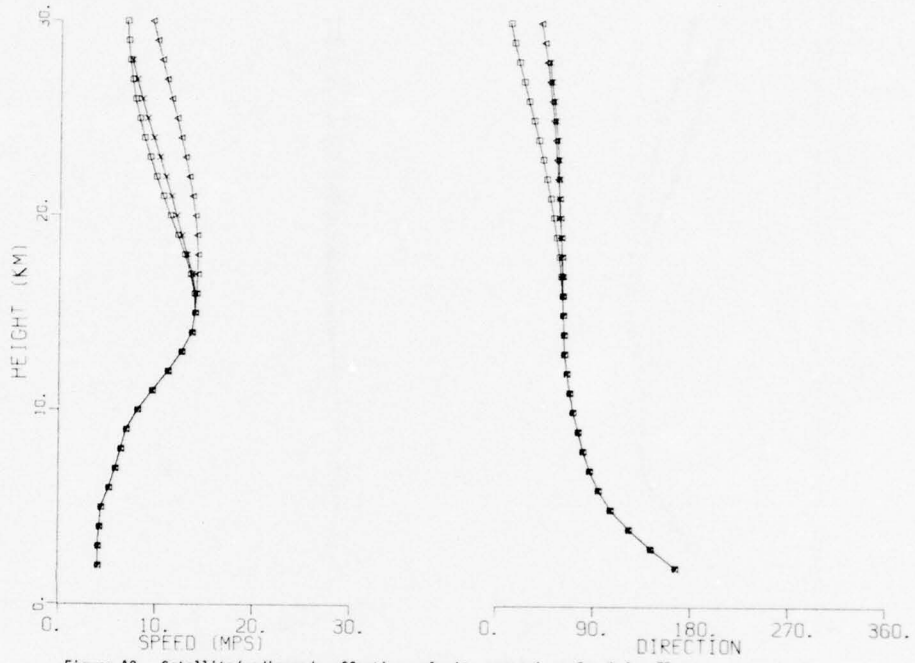


Figure A9. Satellite/radiosonde effective velocity comparison for 9 Jun 75.

5 JUN 75

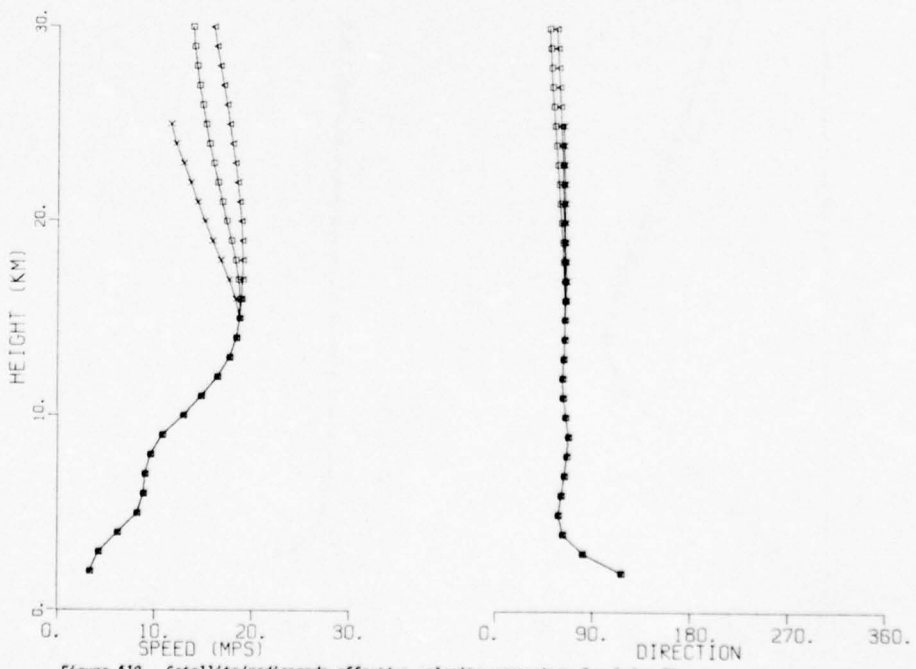


Figure A10. Satellite/radiosonde effective velocity comparison for 5 Jun 75.

BEST AVAILABLE COPY

13 JUN 75

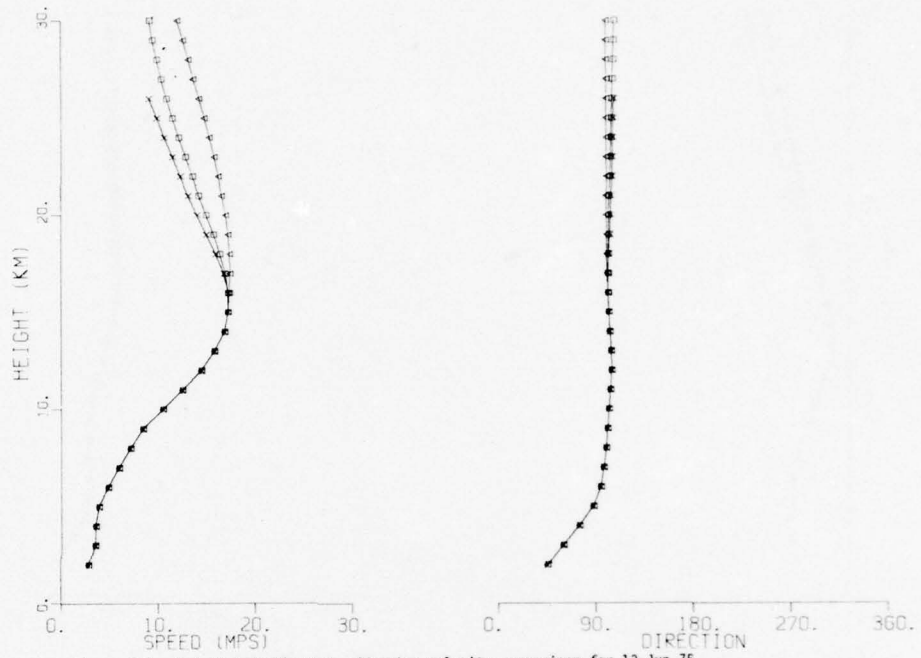


Figure A11. Satellite/radiosonde effective velocity comparison for 13 Jun 75.

17 JUN 75

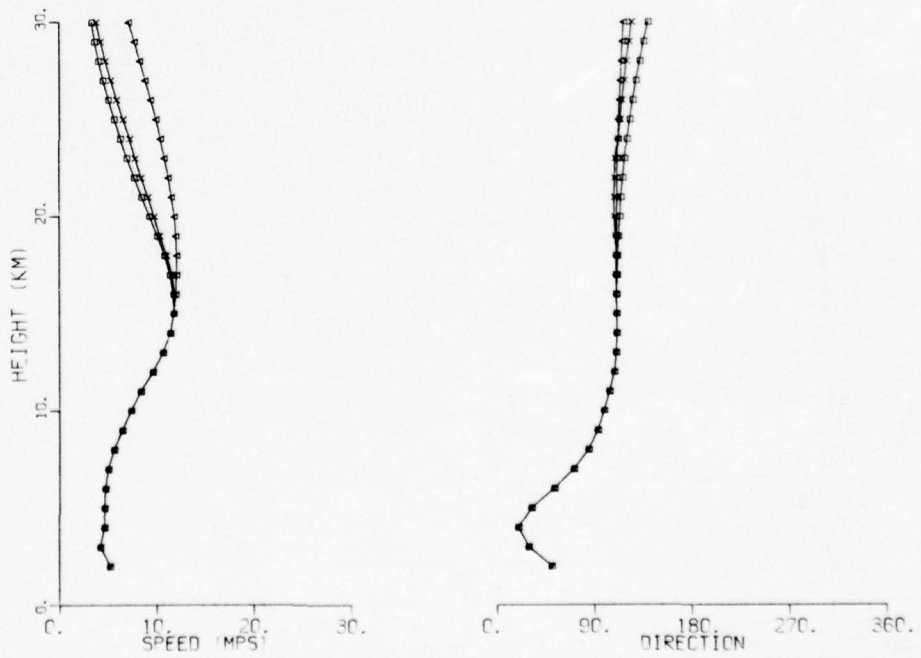


Figure A12. Satellite/radiosonde effective velocity comparison for 17 Jun 75.

BEST AVAILABLE COPY

2 JUL 75

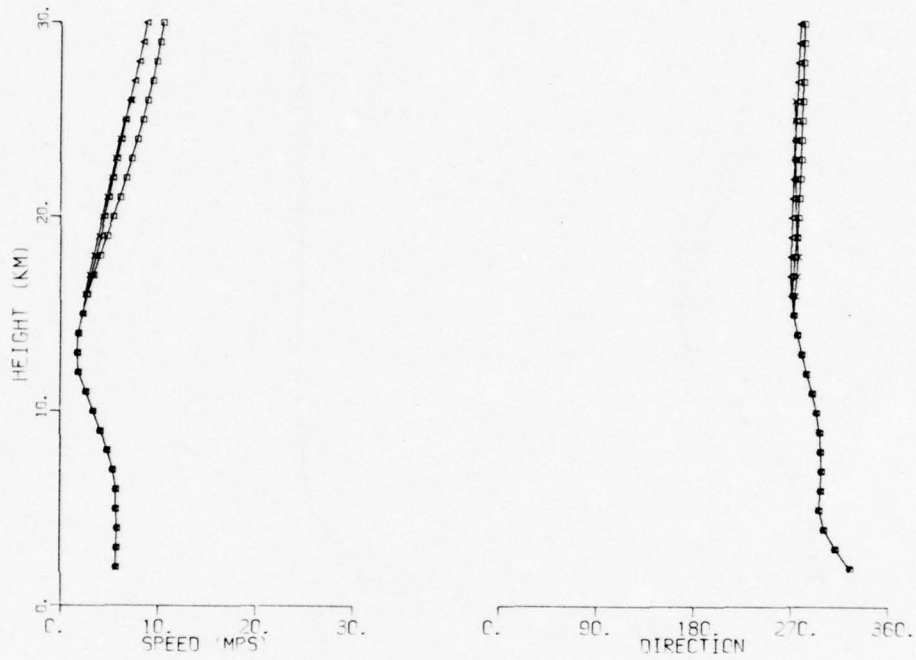


Figure A13. Satellite/radiosonde effective velocity comparison for 2 Jun 75.

23 JUL 75

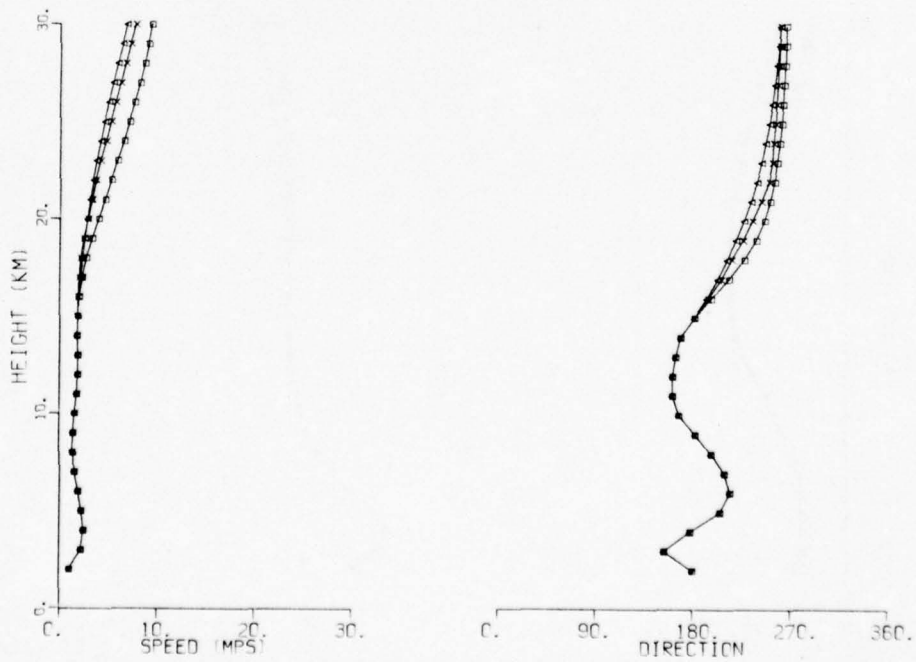


Figure A14. Satellite/radiosonde effective velocity comparison for 23 Jul 75.

4 AUG 75

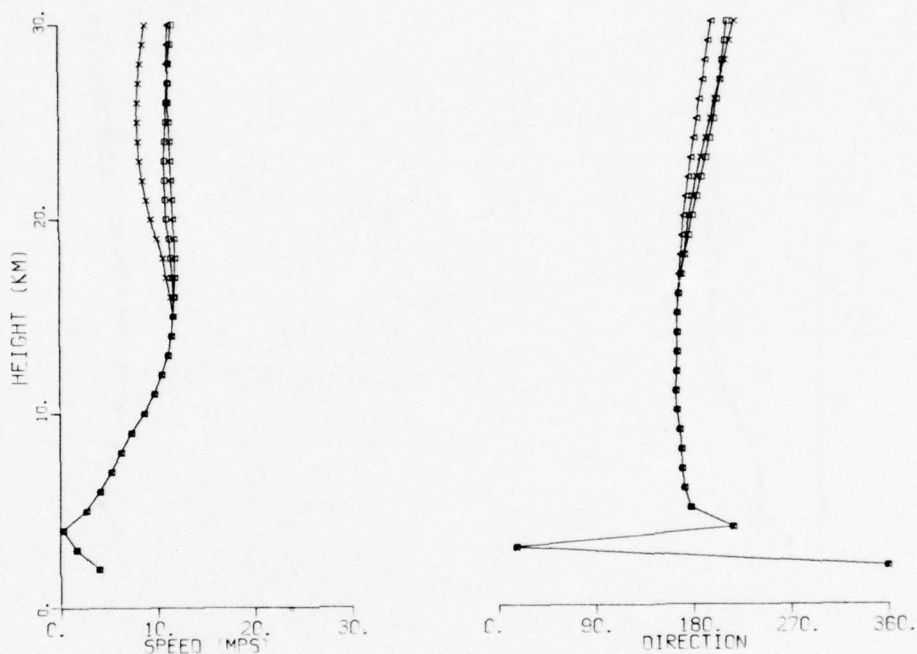


Figure A15. Satellite/radiosonde effective velocity comparison for 4 Aug 75.

6 AUG 75

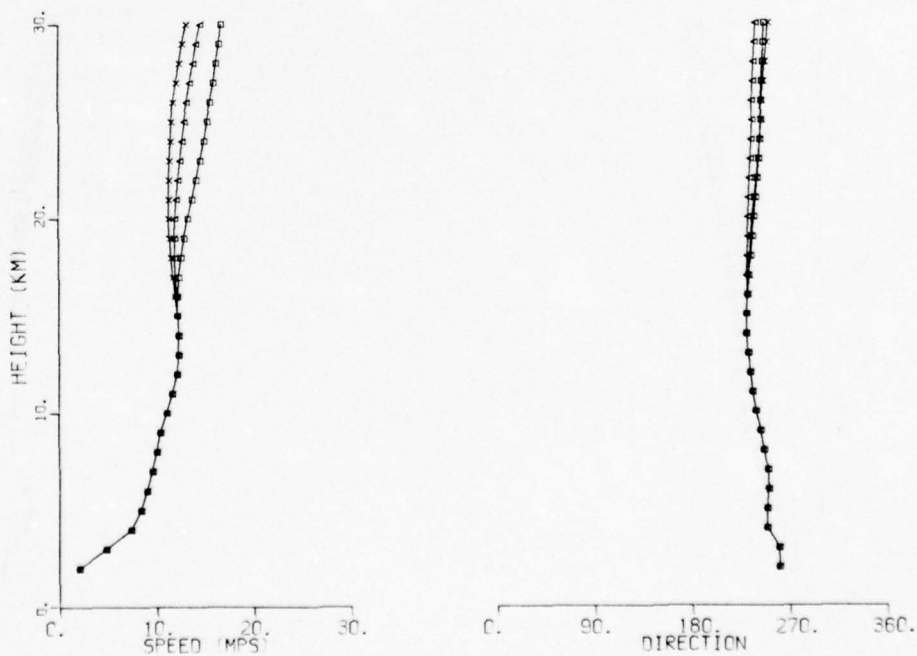


Figure A16. Satellite/radiosonde effective velocity comparison for 6 Aug 75.

7 AUG 75

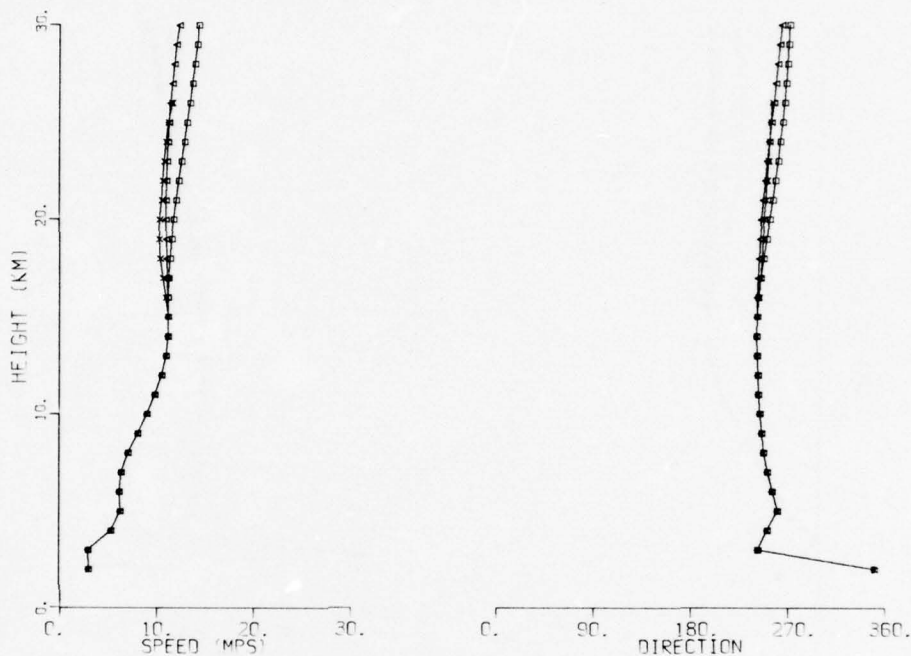


Figure A17. Satellite/radiosonde effective velocity comparison for 7 Aug 75.

19 AUG 75

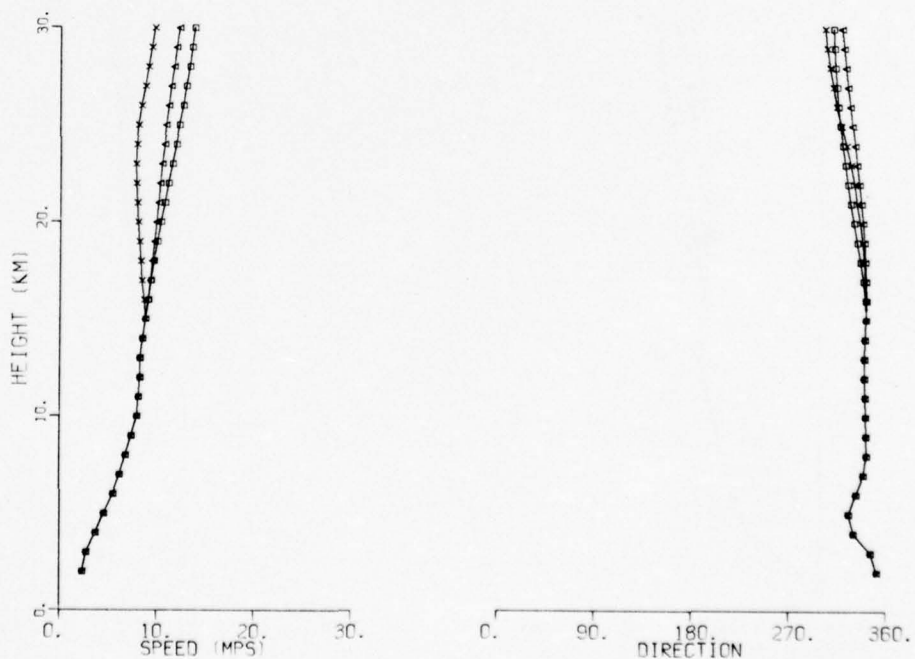


Figure A18. Satellite/radiosonde effective velocity comparison for 19 Aug 75.

9 SEP 75

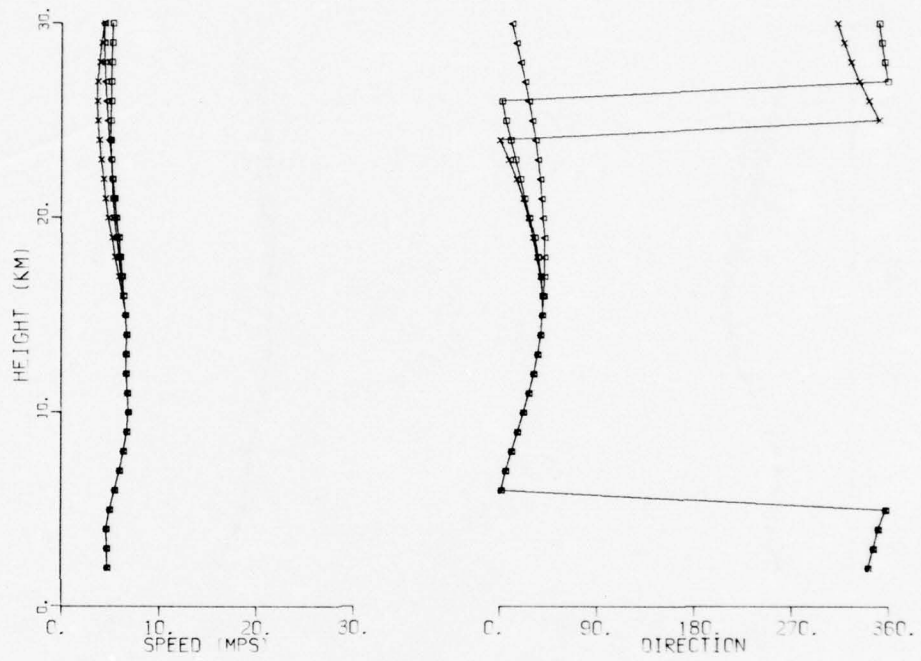


Figure A19. Satellite/radiosonde effective velocity comparison for 9 Sep 75.

11 SEP 75

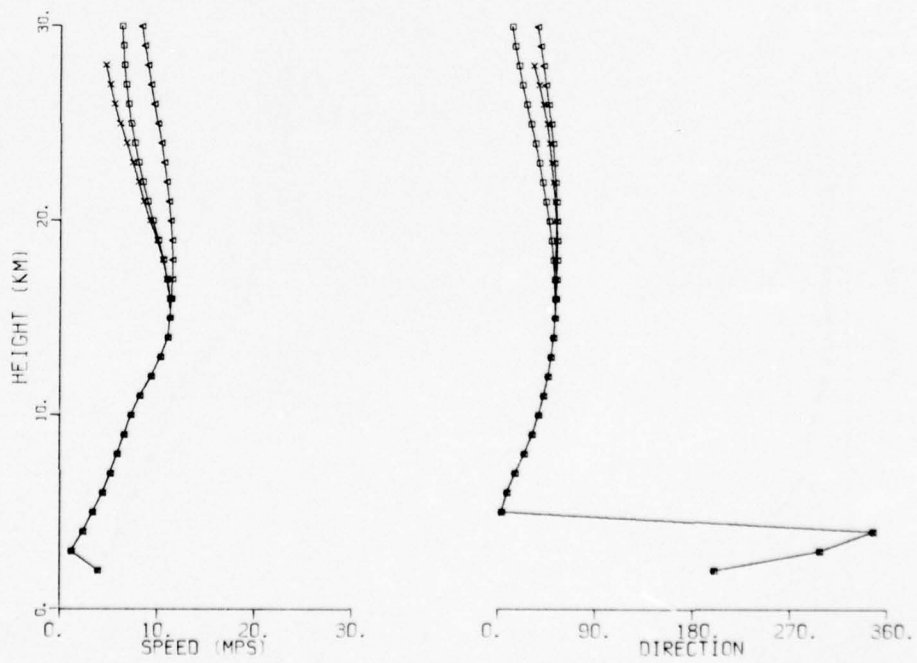


Figure A20. Satellite/radiosonde effective velocity comparison for 11 Sep 75.

19 SEP 75

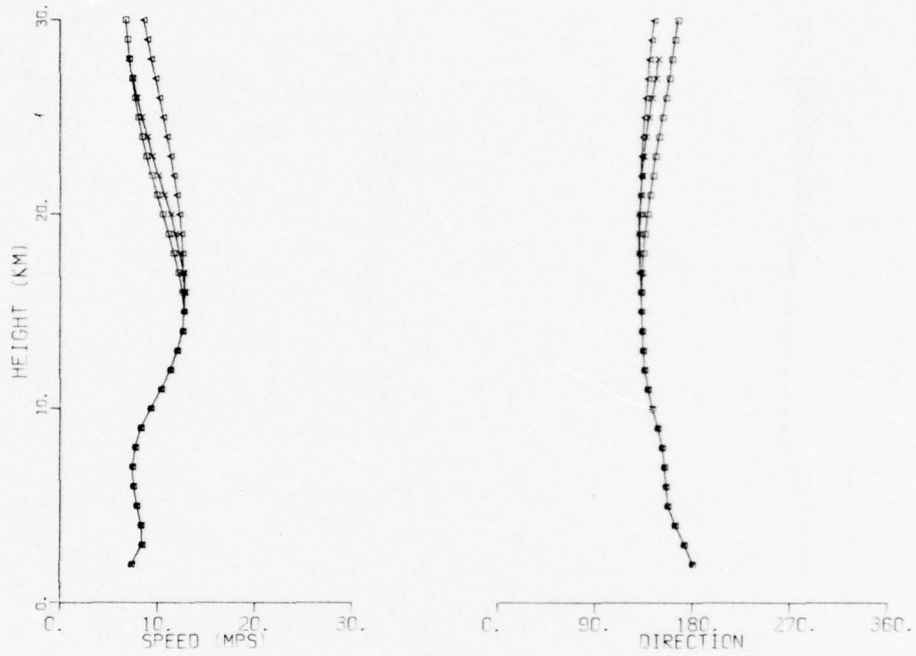


Figure A21. Satellite/radiosonde effective velocity comparison for 19 Sep 75.

24 SEP 75

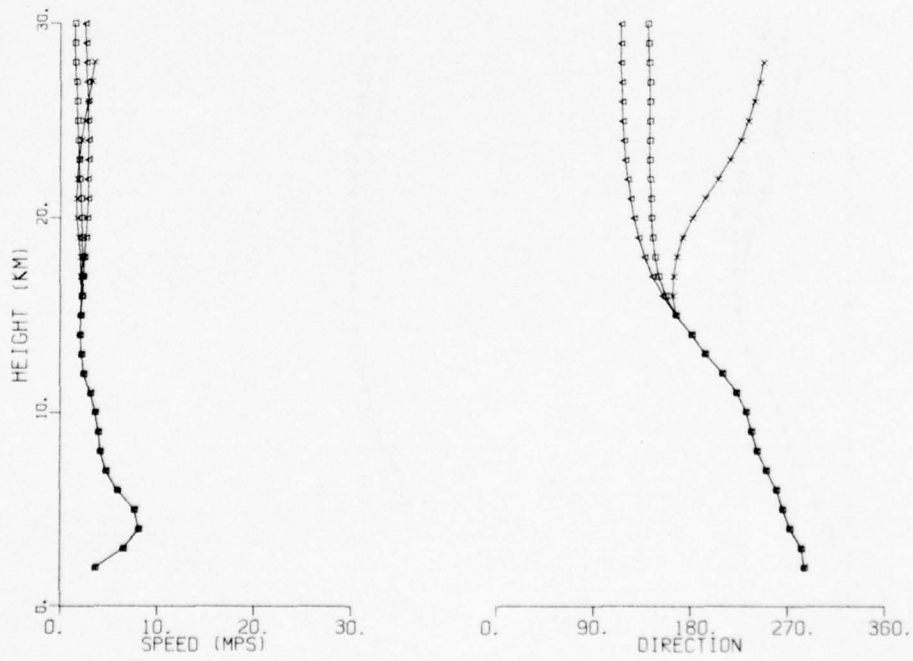


Figure A22. Satellite/radiosonde effective velocity comparison for 24 Sep 75.

26 SEP 75

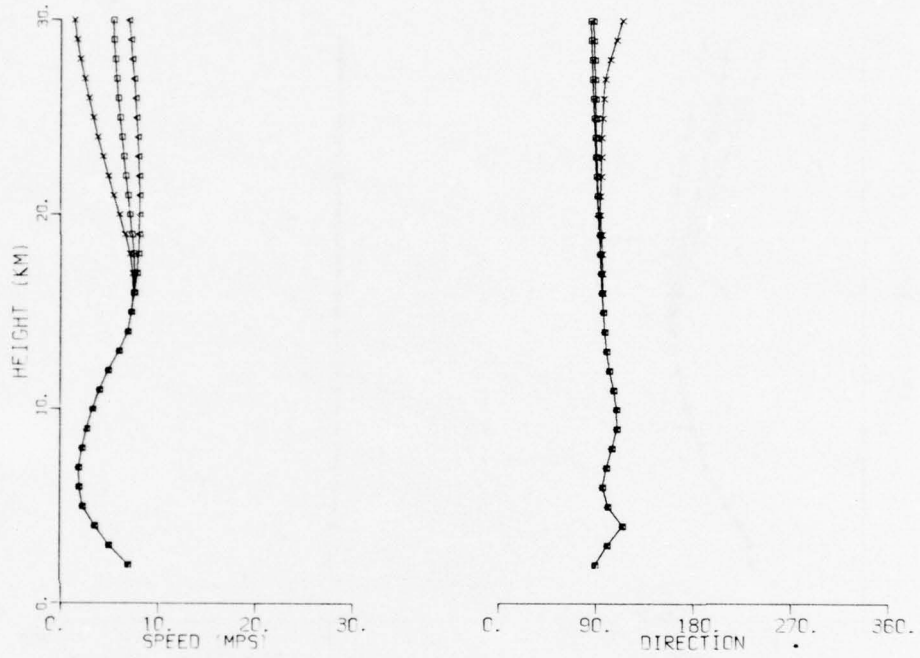


Figure A23. Satellite/radiosonde effective velocity comparison for 26 Sep 75.

2 OCT 75

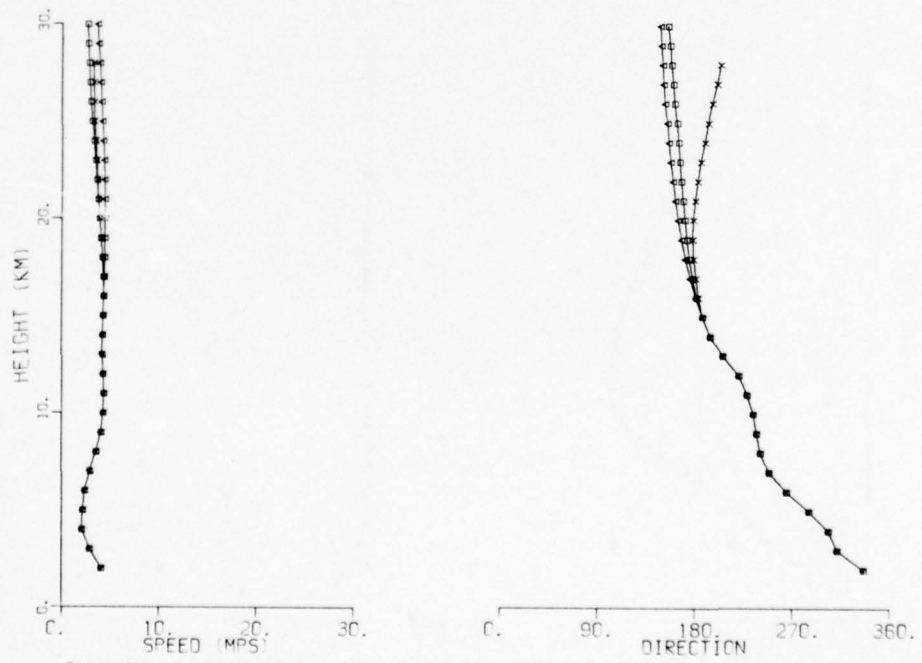


Figure A24. Satellite/radiosonde effective velocity comparison for 2 Oct 75.

8 OCT 75

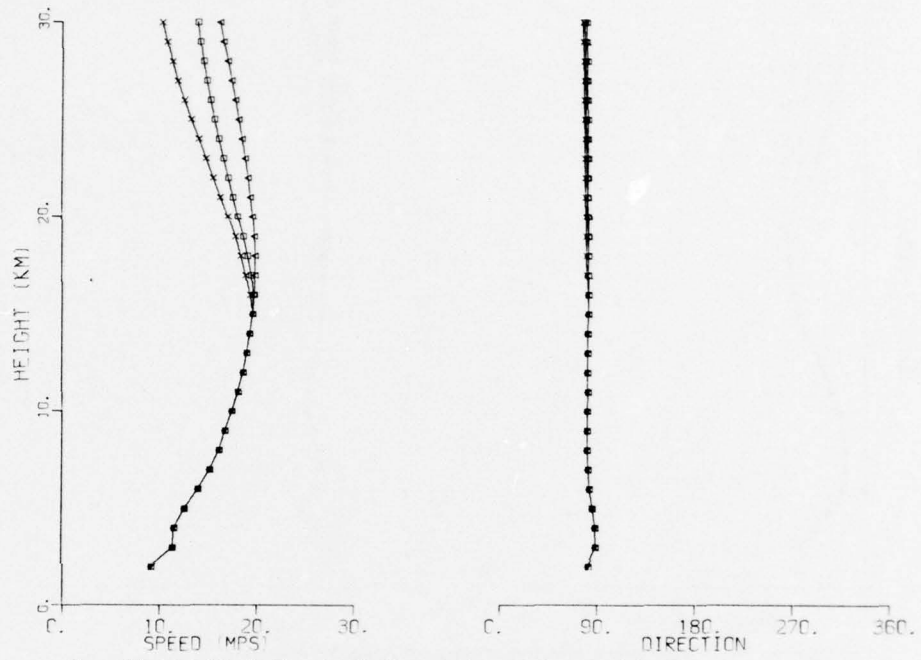


Figure A25. Satellite/radiosonde effective velocity comparison for 8 Oct 75.

14 OCT 75

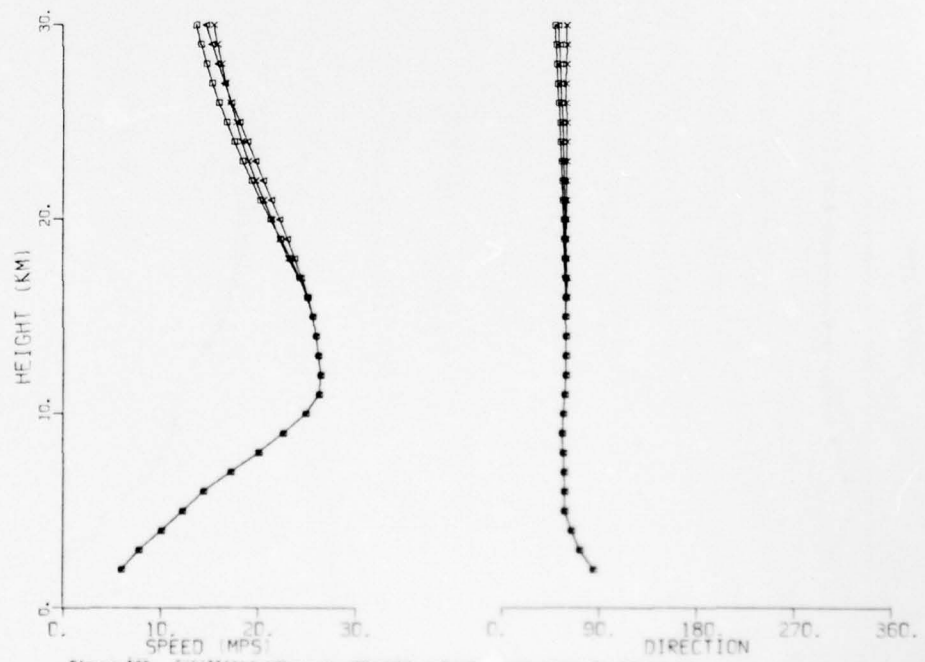


Figure A26. Satellite/radiosonde effective velocity comparison for 14 Oct 75.

29 OCT 75

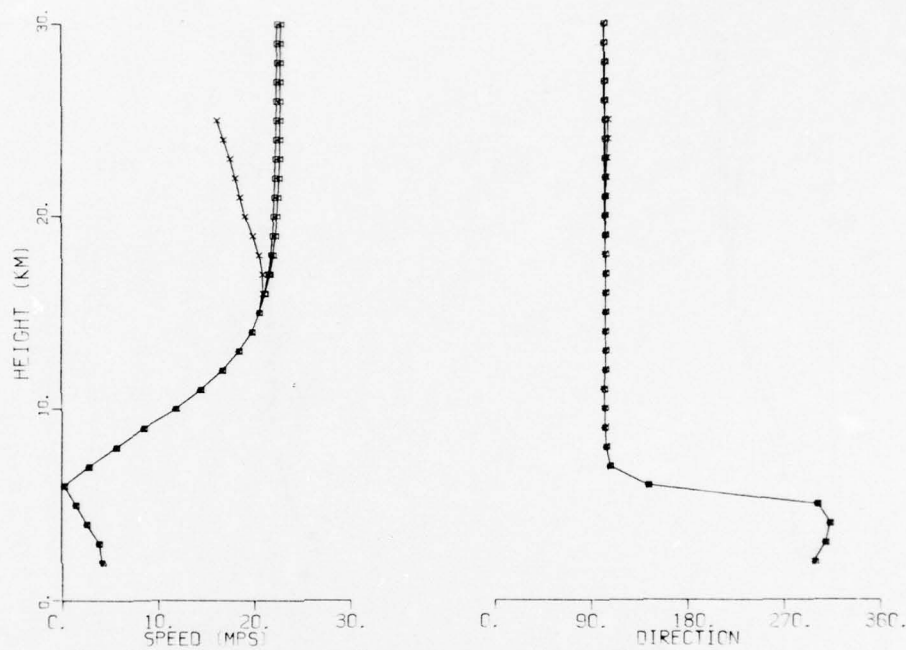


Figure A27. Satellite/radiosonde effective velocity comparison for 29 Oct 75.

6 NOV 75

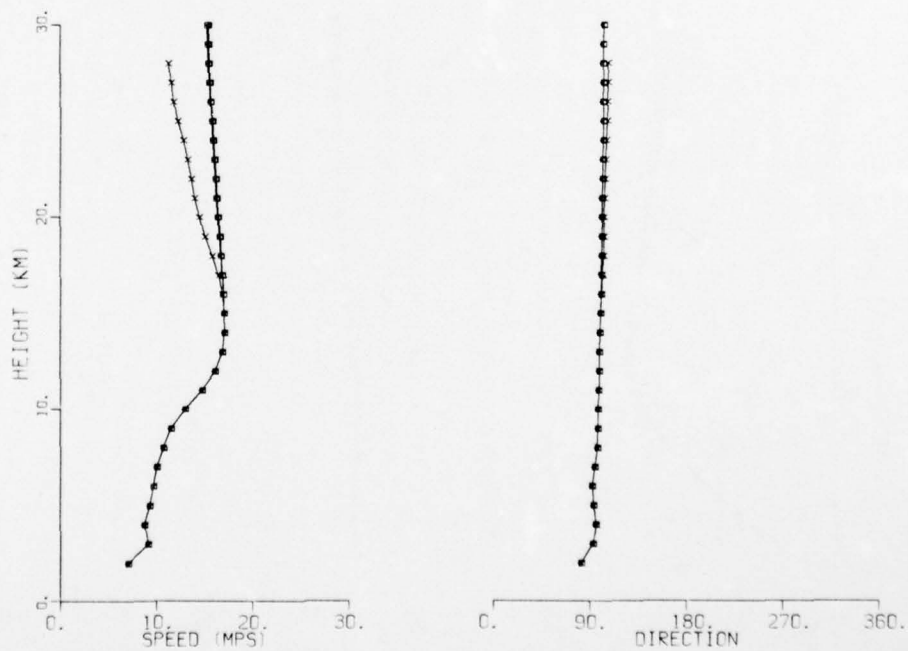


Figure A28. Satellite/radiosonde effective velocity comparison for 6 Nov 75.

13 NOV 75

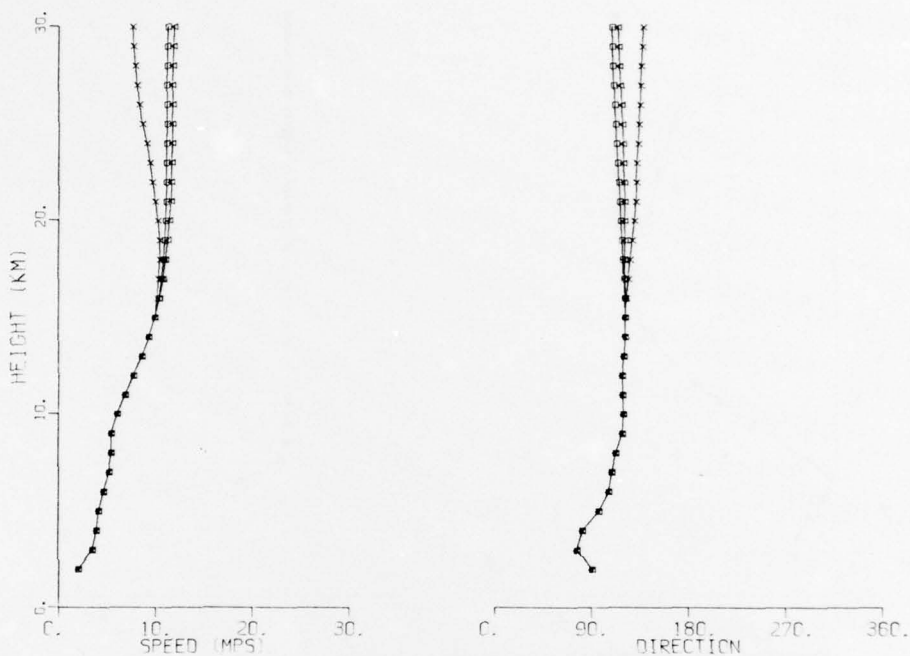


Figure A29. Satellite/radiosonde effective velocity comparison for 13 Nov 75.

4 DEC 75

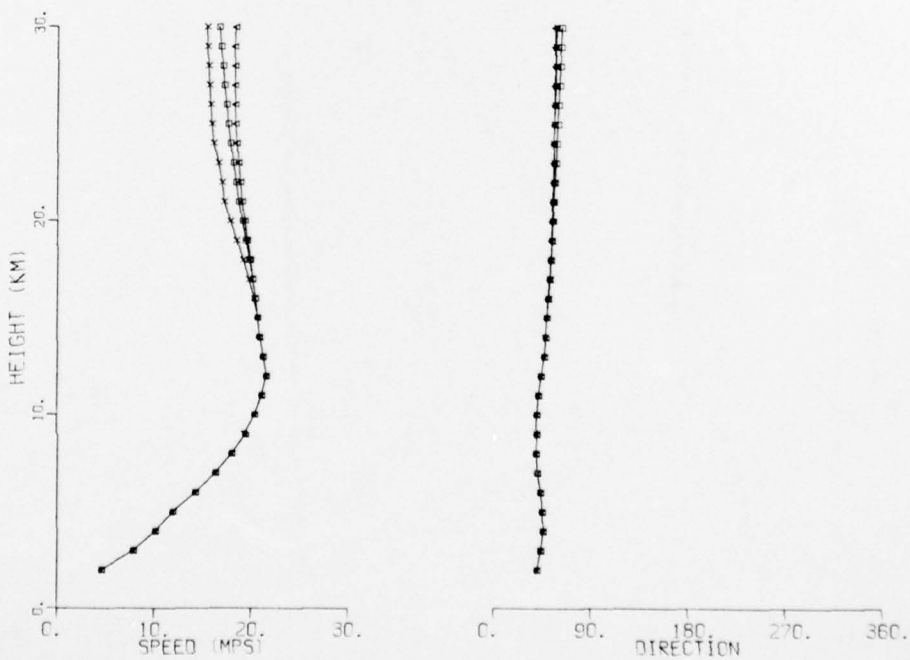


Figure A30. Satellite/radiosonde effective velocity comparison for 4 Dec 75.

10 DEC 75

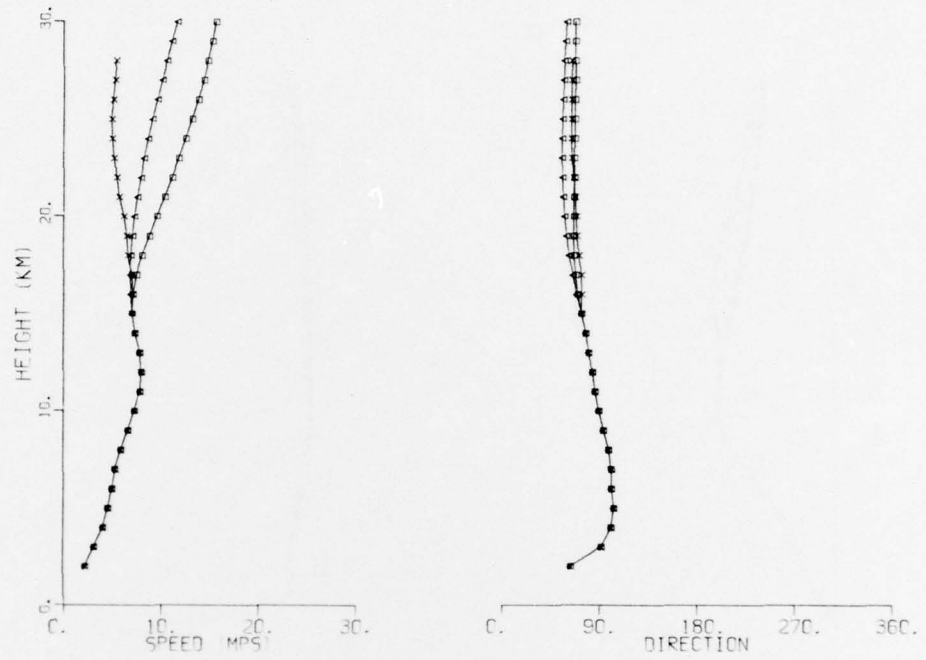


Figure A31. Satellite/radiosonde effective velocity comparison for 10 Dec 75.

12 DEC 75

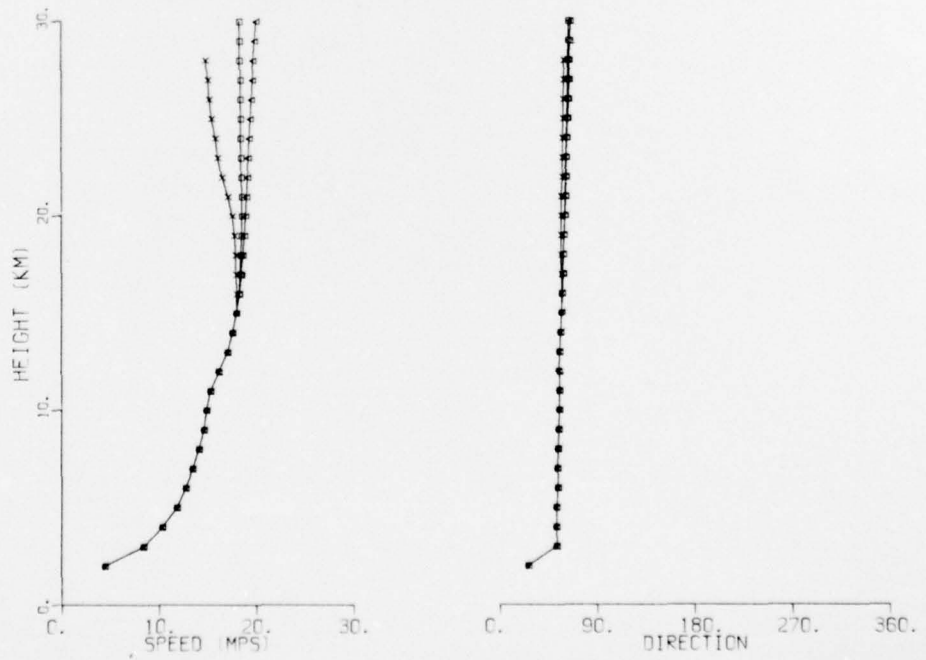


Figure A32. Satellite/radiosonde effective velocity comparison for 12 Dec 75.

18 DEC 75

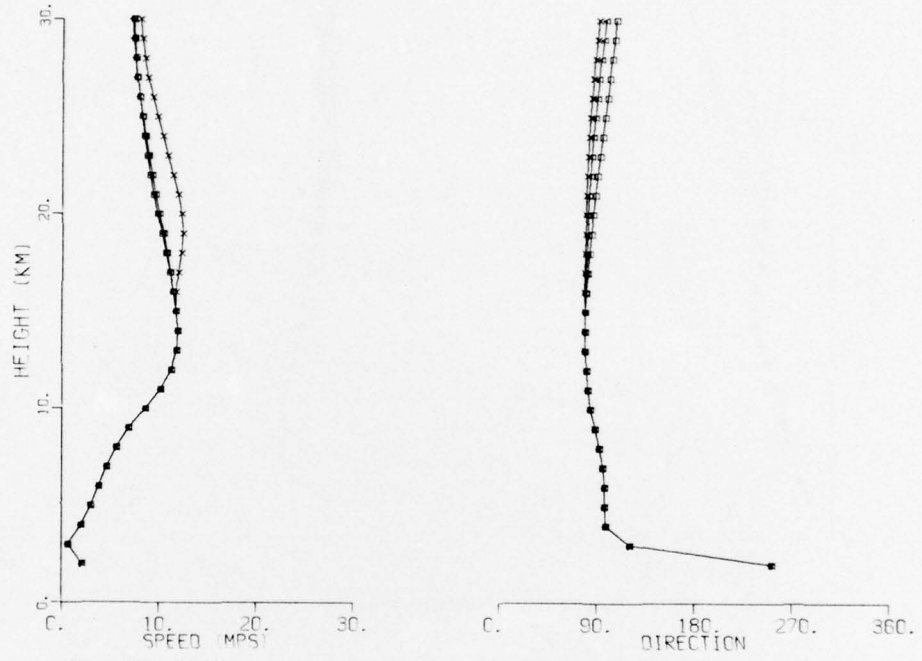


Figure A33. Satellite/radiosonde effective velocity comparison for 18 Dec 75.

ATMOSPHERIC SCIENCES RESEARCH PAPERS

1. Lindberg, J.D., "An Improvement to a Method for Measuring the Absorption Coefficient of Atmospheric Dust and other Strongly Absorbing Powders," ECOM-5565, July 1975.
2. Avara, Elton, P., "Mesoscale Wind Shears Derived from Thermal Winds," ECOM-5566, July 1975.
3. Gomez, Richard B. and Joseph H. Pierluissi, "Incomplete Gamma Function Approximation for King's Strong-Line Transmittance Model," ECOM-5567, July 1975.
4. Blanco, A.J. and B.F. Engebos, "Ballistic Wind Weighting Functions for Tank Projectiles," ECOM-5568, August 1975.
5. Taylor, Fredrick J., Jack Smith, and Thomas H. Pries, "Crosswind Measurements through Pattern Recognition Techniques," ECOM-5569, July 1975.
6. Walters, D.L., "Crosswind Weighting Functions for Direct-Fire Projectiles," ECOM-5570, August 1975.
7. Duncan, Louis D., "An Improved Algorithm for the Iterated Minimal Information Solution for Remote Sounding of Temperature," ECOM-5571, August 1975.
8. Robbiani, Raymond L., "Tactical Field Demonstration of Mobile Weather Radar Set AN/TPS-41 at Fort Rucker, Alabama," ECOM-5572, August 1975.
9. Miers, B., G. Blackman, D. Langer, and N. Lorimier, "Analysis of SMS/GOES Film Data," ECOM-5573, September 1975.
10. Manquero, Carlos, Louis Duncan, and Rufus Bruce, "An Indication from Satellite Measurements of Atmospheric CO₂ Variability," ECOM-5574, September 1975.
11. Petracca, Carmine and James D. Lindberg, "Installation and Operation of an Atmospheric Particulate Collector," ECOM-5575, September 1975.
12. Avara, Elton P. and George Alexander, "Empirical Investigation of Three Iterative Methods for Inverting the Radiative Transfer Equation," ECOM-5576, October 1975.
13. Alexander, George D., "A Digital Data Acquisition Interface for the SMS Direct Readout Ground Station—Concept and Preliminary Design," ECOM-5577, October 1975.
14. Cantor, Israel, "Enhancement of Point Source Thermal Radiation Under Clouds in a Nonattenuating Medium," ECOM-5578, October 1975.
15. Norton, Colburn and Glenn Hoidale, "The Diurnal Variation of Mixing Height by Month over White Sands Missile Range, NM," ECOM-5579, November 1975.
16. Avara, Elton P., "On the Spectrum Analysis of Binary Data," ECOM-5580, November 1975.
17. Taylor, Fredrick J., Thomas H. Pries, and Chao-Huan Huang, "Optimal Wind Velocity Estimation," ECOM-5581, December 1975.
18. Avara, Elton P., "Some Effects of Autocorrelated and Cross-Correlated Noise on the Analysis of Variance," ECOM-5582, December 1975.
19. Gillespie, Patti S., R.L. Armstrong, and Kenneth O. White, "The Spectral Characteristics and Atmospheric CO₂ Absorption of the Ho⁺:YLF Laser at 2.05 μ m," ECOM-5583, December 1975.
20. Novlan, David J., "An Empirical Method of Forecasting Thunderstorms for the White Sands Missile Range," ECOM-5584, February 1976.
21. Avara, Elton P., "Randomization Effects in Hypothesis Testing with Autocorrelated Noise," ECOM-5585, February 1976.
22. Watkins, Wendell R., "Improvements in Long Path Absorption Cell Measurement," ECOM-5586, March 1976.
23. Thomas, Joe, George D. Alexander, and Marvin Dubbin, "SATTEL — An Army Dedicated Meteorological Telemetry System," ECOM-5587, March 1976.
24. Kennedy, Bruce W. and Delbert Bynum, "Army User Test Program for the RDT&E-XM-75

25. Barnett, Kenneth M., "A Description of the Artillery Meteorological Comparisons at White Sands Missile Range, October 1974 - December 1974 ('PASS' - Prototype Artillery [Meteorological] Subsystem)," ECOM-5589, April 1976.
26. Miller, Walter B., "Preliminary Analysis of Fall-of-Shot From Project 'PASS'," ECOM-5590, April 1976.
27. Avara, Elton P., "Error Analysis of Minimum Information and Smith's Direct Methods for Inverting the Radiative Transfer Equation," ECOM-5591, April 1976.
28. Yee, Young P., James D. Horn, and George Alexander, "Synoptic Thermal Wind Calculations from Radiosonde Observations Over the Southwestern United States," ECOM-5592, May 1976.
29. Duncan, Louis D. and Mary Ann Seagraves, "Applications of Empirical Corrections to NOAA-4 VTPR Observations," ECOM-5593, May 1976.
30. Miers, Bruce T. and Steve Weaver, "Applications of Meteorological Satellite Data to Weather Sensitive Army Operations," ECOM-5594, May 1976.
31. Sharenow, Moses, "Redesign and Improvement of Balloon ML-566," ECOM-5595, June 1976.
32. Hansen, Frank V., "The Depth of the Surface Boundary Layer," ECOM-5596, June 1976.
33. Pinnick, R.G. and E.B. Stenmark, "Response Calculations for a Commercial Light-Scattering Aerosol Counter," ECOM-5597, July 1976.
34. Mason, J. and G.B. Hoidale, "Visibility as an Estimator of Infrared Transmittance," ECOM-5598, July 1976.
35. Bruce, Rufus E., Louis D. Duncan, and Joseph H. Pierluissi, "Experimental Study of the Relationship Between Radiosonde Temperatures and Radiometric-Area Temperatures," ECOM-5599, August 1976.
36. Duncan, Louis D., "Stratospheric Wind Shear Computed from Satellite Thermal Sounder Measurements," ECOM-5800, September 1976.
37. Taylor, F., P. Mohan, P. Joseph and T. Pries, "An All Digital Automated Wind Measurement System," ECOM-5801, September 1976.
38. Bruce, Charles, "Development of Spectrophones for CW and Pulsed Radiation Sources," ECOM-5802, September 1976.
39. Duncan, Louis D. and Mary Ann Seagraves, "Another Method for Estimating Clear Column Radiances," ECOM-5803, October 1976.
40. Blanco, Abel J. and Larry E. Traylor, "Artillery Meteorological Analysis of Project Pass," ECOM-5804, October 1976.
41. Miller, Walter and Bernard Engebos, "A Mathematical Structure for Refinement of Sound Ranging Estimates," ECOM-5805, November, 1976.
42. Gillespie, James B. and James D. Lindberg, "A Method to Obtain Diffuse Reflectance Measurements from 1.0 to 3.0 μm Using a Cary 17I Spectrophotometer," ECOM-5806, November 1976.
43. Rubio, Roberto and Robert O. Olsen, "A Study of the Effects of Temperature Variations on Radio Wave Absorption," ECOM-5807, November 1976.
44. Ballard, Harold N., "Temperature Measurements in the Stratosphere from Balloon-Borne Instrument Platforms, 1968-1975," ECOM-5808, December, 1976.
45. Monahan, H.H., "An Approach to the Short-Range Prediction of Early Morning Radiation Fog," ECOM-5809, January 1977.
46. Engebos, Bernard Francis, "Introduction to Multiple State Multiple Action Decision Theory and Its Relation to Mixing Structures," ECOM-5810, January 1977.
47. Low, Richard D.H., "Effects of Cloud Particles on Remote Sensing from Space in the 10-Micrometer Infrared Region, ECOM-5811, January 1977.
48. Bonner, Robert S. and R. Newton, "Application of the AN/GVS-5 Laser Rangefinder to Cloud Base Height Measurements," ECOM-5812, February 1977.

49. Rubio, Roberto, "Lidar Detection of Subvisible Reentry Vehicle Erosive Atmospheric Material," ECOM-5813, March 1977.
50. Low, Richard D.H. and J.D. Horn, "Mesoscale Determination of Cloud-Top Height: Problems and Solutions," ECOM-5814, March 1977.
51. Duncan, Louis D. and Mary Ann Seagraves, "Evaluation of the NOAA-4 VTPR Thermal Winds for Nuclear Fallout Predictions," ECOM-5815, March 1977.

DISTRIBUTION LIST

Commanding Officer
Picatinny Arsenal
ATTN: SARPA-TS-S, #59
Dover, NJ 07801

Chief, Technical Services Div
DCS/Aerospace Sciences
ATTN: AWS/DNTI
Scott AFB, IL 62225

Commanding Officer
Harry Diamond Laboratory
ATTN: Library
2800 Powder Mill Road
Adelphi, MD 20783

Air Force Cambridge Rsch Labs
ATTN: LCH (A. S. Carten, Jr.)
Hanscom AFB
Bedford, MA 01731

Commander
US Army Electronics Command
ATTN: DRSEL-RD-D
Fort Monmouth, NJ 07703

Department of the Air Force
16WS/DO
Fort Monroe, VA 23651

Naval Surface Weapons Center
Code DT 21 (Ms. Greeley)
Dahlgren, VA 22448

Director
US Army Ballistic Research Lab
ATTN: DRXBR-AM
Aberdeen Proving Ground, MD 21005

Air Force Weapons Laboratory
ATTN: Technical Library (SUL)
Kirtland AFB, NM 87117

Geophysics Division
Code 3250
Pacific Missile Test Center
Point Mugu, CA 93042

Director
US Army Engr Waterways Exper Sta
ATTN: Library Branch
Vicksburg, MS 39180

National Center for Atmos Res
NCAR Library
PO Box 3000
Boulder, CO 80303

Commander
US Army Electronics Command
ATTN: DRSEL-CT-D
Fort Monmouth, NJ 07703

William Peterson
Research Association
Utah State University, UNC 48
Logan, UT 84322

Meteorologist in Charge
Kwajalein Missile Range
PO Box 67
APO
San Francisco, CA 96555

Commander
US Army Dugway Proving Ground
ATTN: MT-S
Dugway, UT 84022

Environmental Protection Agency
Meteorology Laboratory
Research Triangle Park, NC 27711

Head, Rsch and Development Div (ESA-131)
Meteorological Department
Naval Weapons Engineering Support Act
Washington, DC 20374

Commander
US Army Engineer Topographic Lab
(STINFO CENTER)
Fort Belvoir, VA 22060

Commander
US Army Electronics Command
ATTN: DRSEL-MS-TI
Fort Monmouth, NJ 07703

Commander
US Army Missile Command
ATTN: DRSMI-RRA, Bldg 7770
Redstone Arsenal, AL 35809

Commander
US Army Electronics Command
ATTN: DRSEL-GG-TD
Fort Monmouth, NJ 07703

Air Force Avionics Lab
ATTN: AFAL/TSR
Wright-Patterson AFB, Ohio 45433

Dr. Robert Durrenberger
Dir, The Lab of Climatology
Arizona State University
Tempe, AZ 85281

Commander
US Army Electronics Command
ATTN: DRSEL-VL-D
Fort Monmouth, NJ 07703

Commander
Headquarters, Fort Huachuca
ATTN: Tech Ref Div
Fort Huachuca, AZ 85613

Commander
USAICS
ATTN: ATSI-CTD-MS
Fort Huachuca, AZ 85613

Field Artillery Consultants
1112 Becontree Drive
ATTN: COL Buntyn
Lawton, OK 73501

E&R Center
Bureau of Reclamation
ATTN: Bldg 67, Code 1210
Denver, CO 80225

Commander
US Army Nuclear Agency
ATTN: ATCA-NAW
Building 12
Fort Bliss, TX 79916

HQDA (DAEN-RDM/Dr. De Percin)
Forrestal Bldg
Washington, DC 20314

Director
Atmospheric Physics & Chem Lab
Code 31, NOAA
Department of Commerce
Boulder, CO 80302

Commander
Air Force Weapons Laboratory
ATTN: AFWL/WE
Kirtland AFB, NM 87117

Dr. John L. Walsh
Code 5503
Navy Research Lab
Washington, DC 20375

Commander
US Army Satellite Comm Agc
ATTN: DRCPM-SC-3
Fort Monmouth, NJ 07703

Commander
US Army Electronics Command
ATTN: DRCDE-R
5001 Eisenhower Avenue
Alexandria, VA 22304

Marine Corps Dev & Educ Cmd
Development Center
ATTN: Cmd, Control, & Comm Div (C³)
Quantico, VA 22134

Commander
US Army Electronics Command
ATTN: DRSEL-WL-D1
Fort Monmouth, NJ 07703

Commander
US Army Missile Command
ATTN: DRSMI-RFGA, B. W. Fowler
Redstone Arsenal, AL 35809

Dir of Dev & Engr
Defense Systems Div
ATTN: SAREA-DE-DDR
H. Tannenbaum
Edgewood Arsenal, APG, MD 21010

Mr. William A. Main
USDA Forest Service
1407 S. Harrison Road
East Lansing, MI 48823

Naval Surface Weapons Center
Technical Library and Information
Services Division
White Oak, Silver Spring, MD 20910

Dr. A. D. Belmont
Research Division
PO Box 1249
Control Data Corp
Minneapolis, MN 55440

Dir, Elec Tech and Devices Lab
US Army Electronics Command
ATTN: DRSEL-TL-D, Bldg 2700
Fort Monmouth, NJ 07703

Director
Development Center MCDEC
ATTN: Firepower Division
Quantico, VA 22134

Commander
US Army Proving Ground
ATTN: Technical Library, Bldg 2100
Yuma, AZ 85364

US Army Liaison Office
MIT-Lincoln Lab, Library A-082
PO Box 73
Lexington, MA 02173

Library-R-51-Tech Reports
Environmental Research Labs
NOAA
Boulder, CO 80302

Head, Atmospheric Research Section
National Science Foundation
1800 G. Street, NW
Washington, DC 20550

Commander
US Army Missile Command
ATTN: DRSMI-RR
Redstone Arsenal, AL 35809

Commandant
US Army Field Artillery School
ATTN: Met Division
Fort Sill, OK 73503

Meteorology Laboratory
AFCRL/LY
Hanscom AFB
Bedford, MA 01731

Commander
US Army Air Defense School
ATTN: C&S Dept, MSLSCI Div
Fort Bliss, TX 79916

Director National Security Agency
ATTN: TDL (C513)
Fort George G. Meade, MD 20755

USAF EPAC/CBT (Stop 825)
ATTN: Mr. Burgmann
Scott AFB, IL 62225

Armament Dev & Test Center
ADTC (DLOSL)
Eglin AFB, Florida 32542

Commander
US Army Ballistic Rsch Labs
ATTN: DRXBR-IB
Aberdeen Proving Ground, MD 21005

Director
Naval Research Laboratory
Code 2627
Washington, DC 20375

Commander
Naval Elect Sys Cmd HQ
Code 51014
Washington, DC 20360

The Library of Congress
ATTN: Exchange & Gift Div
Washington, DC 20540
2

CO, US Army Tropic Test Center
ATTN: STETC-MO-A (Tech Lib)
APO New York 09827

Commander
Naval Electronics Lab Center
ATTN: Library
San Diego, CA 92152

Office, Asst Sec Army (R&D)
ATTN: Dep for Science & Tech
Hq, Department of the Army
Washington, DC 20310

Director
US Army Ballistic Research Lab
ATTN: DRXBR-AM, Dr. F. E. Niles
Aberdeen Proving Ground, MD 21005

Commander
Frankford Arsenal
ATTN: Library, K2400, Bldg 51-2
Philadelphia, PA 19137

Director
US Army Ballistic Research Lab
ATTN: DRXBR-XA-LB
Bldg 305
Aberdeen Proving Ground, MD 21005

Dir, US Naval Research Lab
Code 5530
Washington, DC 20375

Commander
Office of Naval Research
Code 460-M
Arlington, VA 22217

Commander
Naval Weather Service Command
Washington Navy Yard
Bldg 200, Code 304
Washington, DC 20374

Technical Processes Br
D823
Room 806, Libraries Div NOAA
8060 13th St
Silver Spring, MD 20910

The Environmental Rsch Institute of MI
ATTN: IRIA Library
PO Box 618
Ann Arbor, MI 48107

Redstone Scientific Info Center
ATTN: Chief, Documents
US Army Missile Command
Redstone Arsenal, AL 35809

Commander
Edgewood Arsenal
ATTN: SAREA-TS-L
Aberdeen Proving Ground, MD 21010

Sylvania Elec Sys Western Div
ATTN: Technical Reports Library
PO Box 205
Mountain View, CA 94040

Commander
US Army Security Agency
ATTN: IARD-OS
Arlington Hall Station
Arlington, VA 22212
2

President
US Army Field Artillery Board
Fort Sill, OK 73503

Commandant
US Army Field Artillery School
ATTN: ATSF-TA-R
Fort Sill, OK 73503

CO, USA Foreign Sci & Tech Center
ATTN: DRXST-ISI
220 7th Street, NE
Charlottesville, VA 22901

Commander, Naval Ship Sys Cmd
Technical Library, Rm 3 S-08
National Center No. 3
Washington, DC 20360

Commandant
US Army Signal School
ATTN: ATSN-CD-MS
Fort Gordon, GA 30905

Rome Air Development Center
ATTN: Documents Library
TILD (Bette Smith)
Griffiss Air Force Base, NY 13441

HQ, ESD/DRI/S-22
Hanscom AFB
MA 01731

Commander
Frankford Arsenal
ATTN: J. Helfrich PDSP 65-1
Philadelphia, PA 19137

Director
Defense Nuclear Agency
ATTN: Tech Library
Washington, DC 20305

Department of the Air Force
5WW/DOX
Langley AFB, VA 23665

Commander
US Army Missile Command
ATTN: DRSMI-RER (Mr. Haraway)
Redstone Arsenal, AL 35809

CPT Hugh Albers, Exec Sec
Interdept Committee on Atmos Sci
Fed Council for Sci & Tech
National Sci Foundation
Washington, DC 20550

US Army Research Office
ATTN: DRXRO-IP
PO Box 12211
Research Triangle Park, NC 27709

Dr. Frank D. Eaton
PO Box 3038
University Station
Laramie, Wyoming 82071

Commander
US Army Training & Doctrine Cmd
ATTN: ATCD-SC
Fort Monroe, VA 23651

Commander
US Army Arctic Test Center
ATTN: STEAC-OP-PL
APO Seattle 98733

Mil Assistant for Environmental Sciences
OAD (E & LS), 3D129
The Pentagon
Washington, DC 20301

Commander
US Army Electronics Command
ATTN: DRSEL-GS-H (Stevenson)
Fort Monmouth, NJ 07703

Commander
Eustis Directorate
US Army Air Mobility R&D Lab
ATTN: Technical Library
Fort Eustis, VA 23604

Commander
USACACDA
ATTN: ATCA-CCC-W
Fort Leavenworth, KS 66027

National Weather Service
National Meteorological Center
World Weather Bldg - 5200 Auth Rd
ATTN: Mr. Quiroz
Washington, DC 20233

Commander
US Army Test & Eval Cmd
ATTN: DRSTE-FA
Aberdeen Proving Ground, MD 21005

Commander
US Army Materiel Command
ATTN: DRCRD-SS (Mr. Andrew)
Alexandria, VA 22304

Air Force Cambridge Rsch Labs
ATTN: LKI
L. G. Hanscom Field
Bedford, MA 01730

Commander
Frankford Arsenal
ATTN: SARFA-FCD-O, Bldg 201-2
Bridge & Tarcony Sts
Philadelphia, PA 19137

Director, Systems R&D Service
Federal Aviation Administration
ATTN: ARD-54
2100 Second Street, SW
Washington, DC 20590

Inge Dirmhirn, Professor
Utah State University, UMC 48
Logan, UT 84322

USAFETAC/CB (Stop 825)
Scott AFB
IL 62225

Chief, Aerospace Environ Div
Code ES41
NASA
Marshall Space Flight Center, AL 35802

Director
USAE Waterways Experiment Station
ATTN: Library
PO Box 631
Vicksburg, MS 39180

Defense Documentation Center
ATTN: DDC-TCA
Cameron Station (BLDG 5)
Alexandria, Virginia 22314
12

Commander
US Army Electronics Command
ATTN: DRSEL-CT-S
Fort Monmouth, NJ 07703

Commander
Holloman Air Force Base
6585 TG/WE
Holloman AFB, NM 88330

Commandant
USAFAS
ATTN: ATSF-CD-MT (Mr. Farmer)
Fort Sill, OK 73503
2

Commandant
USAFAS
ATTN: ATSF-CD-C (Mr. Shelton)
Fort Sill, OK 73503
2

Commander
US Army Electronics Command
ATTN: DRSEL-CT-S (Dr. Swingle)
Fort Monmouth, NJ 07703
3